Robust Nonlinear Path-Following Control of an AUV

Lionel Lapierre and Bruno Jouvencel

***Abstract*—This paper develops a robust nonlinear controller that asymptotically drives the dynamic model of an autonomous underwater vehicle (AUV) onto a predefined path at a constant forward velocity. A kinematic controller is first derived, and extended to cope with vehicle dynamics by resorting to backstepping and Lyapunov-based techniques. Robustness to vehicle parameter uncertainty is addressed by incorporating a hybrid parameter adaptation scheme. The resulting nonlinear adaptive control system is formally shown and it yields asymptotic convergence of the vehicle to the path. Simulations illustrate the performance of the derived controller.**

***Index Terms*—Adaptive control, nonlinear control, path following, underactuated vehicle.**

I. Introduction

THE design of a nonlinear path-following controller autonomous underwater vehicle (AUV) involves two different problems: the path-following strategy and the control of an underactuated vehicle.

A. Path Following

Path following requires the vehicle to reach and follow a desired path without time constraint. This is done by controlling the forward velocity to converge to a desired value (constant in our case), and acting on the vehicle's orientation to drive it onto the path. The problem is considered to be solved when the designed controller guarantees asymptotic convergence to the path. Many papers have addressed the problem of path-following control for a nonholonomic wheeled vehicle, in most cases a unicycle-type robot [25], [33], [34]. The underlying questions to be solved concern the following.

1) *Path parameterization.* If the path can be considered as straight lines or circles, classic geometrical description may be used to parameterize the path and in the control design [22], [28], [31]. The most general parameterization considers the curvature of the path in function of the curvilinear abscissa of the target point [20], [33], [34].
2) *Choice of the target point on the path.* The choice of the target point implies different control strategies. In [33], the target point is designed to be the closest point on the path, relative to the current position of the robot. This allows a rapid convergence to the path, since the distance to the path is minimal. However, this method implies a drastic limitation to the robot's initial conditions. Since the target point is defined with respect to the current position of the robot, it has to be actualized at each instant of time, and problems occur when the robot is located at the center of the path curvature (the target point is no longer unique) or during a movement that potentially passes close to it (the computation of the current reference is not well posed). To solve this problem, a very conservative but necessary condition is used: the initial position of the robot must be such that the initial distance to the path is *smaller than the smallest radius of curvature present on the path*. Another solution [24], [39] consists in considering the target point as a virtual moving target, animated on the path with its own movement laws. To ensure cooperative behavior of the target (slowing down when the vehicle is behind and accelerating when the vehicle is in advance), the movement equations of the target are related to the velocity of the robot. This implies that the target exponentially converges to the closest point on the path, with the difference that the target point is now well defined, even if the vehicle crosses the current center of curvature. The previous constraint is relaxed into the following: the initial position of the vehicle should be*far from the center of curvature relative to the initial position of the target point on the path*.

B. Control of an Underactuated Vehicle

An increasing number of papers have addressed the topic of the control of ocean vehicles. Vehicles designed to accomplish long-range missions (AUVs, ships) are generally underactuacted, or in the case of fully actuated vehicles, the inefficiency of a side thruster during high-velocity forward movement leads them to be considered as underactuated. This implies that transverse movement (sway) is not directly controlled.

In the case of a wheeled robot, the transverse ground friction of the wheels, expressing the nonholonomic constraint, effectively cancels this behavior. Nevertheless, in underwater or terrestrial plane applications, the control inputs are the same: the forward and yaw velocities. This explains the connection between unicycle-type robots and AUV path-following control strategies. For a unicycle-type robot path-following control, please refer to [31], [33], [34], and [23].

The similarity between these two vehicles ends on considering that the resulting total velocity of the underwater robot is not aligned with its main direction of movement. This implies that the AUV heading is not permanently tangent to its trajectory, but the strategy of controlling the amplitude and the orientation of the total velocity holds, underlying the added necessity of having a measurement, or a satisfactory estimation,

Manuscript received January 5, 2006; revised May 31, 2007; accepted February 26, 2008. This work was supported by the EC under Project FREESUB***[AU: Please define EC and FREESUB]***.

Associate Editor: D. Stilwell.

The authors are with the Laboratoire d'Informatique de Robotique et de Microélectronique de Montpellier (LIRMM) Institute, Montpellier 34392, France (e-mail: lapierre@lirmm.fr).

Color versions of one or more of the figures in this paper are available online at http://ieeexplore.ieee.org.

Digital Object Identifier 10.1109/JOE.2008.923554

of the sway velocity [21], [26]. Path-following systems for marine vehicles have been reported by Encarnacao *et al.* in [18], and [19], where the underlying assumption was that the vehicle's forward speed tracks a desired speed profile, while the controller acts on the vehicle's orientation to drive it to the path***[AU: "speed" and "velocity" are used interchangeably in the paper. Can "speed" be used throughout?]***. Typically, smoother convergence to a path is achieved, in comparison with performances obtained with a trajectory-tracking controller, and the control signals are less often pushed to saturation [17].

Because the AUV controller relies on a dynamic model of the system, the performances achieved are dependent on the accuracy of the estimation of model parameters. Nevertheless, precise modeling for an AUV is a difficult task, and it results in a set of highly coupled nonlinear equations. For more information on a subject of modeling, the reader should refer to [16] and [15].

Designing a controller to regulate such a nonlinear model is not a simple process, and classic linear approaches do not lead to satisfactory performances [14]. Meanwhile, Silvestre *et al.* [13] propose a gain-scheduled trajectory-tracking controller, based on the fact that the linearization of the system dynamics about trimming trajectory (helices parameterized by the vehicle's linear speed, yaw rate, and flight path angle) results in a time-invariant plant. Then, considering a global trajectory consisting of the piecewise union of trimming trajectories, the problem is solved by designing a family of linear controllers for the linearized plants at each operating point. Interpolating between these controllers guarantees adequate local performance for all linearized plants. Nevertheless, this methodology does not explicitly address the issues of global stability and performance.

Because model estimation accuracy cannot be absolutely guaranteed, the robustness of the control scheme is of major importance. One of the classic control methods relies on the sliding-mode design [12]. In [11], Salgado *et al.* propose a control design applied to the Taipan 2 AUV, based on an high-order sliding mode, that explicitly addresses the classic chattering problem encountered when using the classic sliding mode. This is achieved by controlling high-order derivatives of the sliding surface, thus removing the discontinuity of the control vector. This method exhibits robust behavior, but the equivalent control is designed using a linearized method that does not allow for global stability and performance analysis. In [8], Song *et al.* combine the sliding-mode advantages with a fuzzy approach expressing the switching rules based on the experimental data. The authors say this method is independent of any system model. Nevertheless, global stability and performance are not addressed. Naem *et al.* [10] and [9] propose a control based on model prediction using genetic algorithms, but the performances and stability properties are not addressed.

Considering model nonlinearities, the Lyapunov approach has many advantages. The first step allows for designing a control solution that takes into account the system kinematics and meets uniform asymptotic convergence requirements. As we will see in the sequel, the concurrent use of the virtual target principle allows for expressing the problem in a nonsingular way, thus guaranteeing the respect of the convergence property whatever the initial conditions are, and meeting a global and uniform asymptotic convergence requirement. The second step consists in using the backstepping approach [7], augmenting the system with its dynamic states, and still meeting global performance requirements. For an application of this method to an underactuacted marine system, please refer to [17]. Another backstepping stage allows parameter uncertainty to be taken into account, in designing an adaptive scheme that guarantees robustness. It should be noted that this method is valid if the parameters appear in an affine form in the control expression. An application to a nonholonomic wheeled system can be found in [4]. The particularity of an AUV system is its underactuation, which leads to a Lyapunov-based control expression, with parameters that do not appear in an affine form [6]. Existing solutions are based on a model simplification, reducing the problem to a multivariable linear system [5], [15], [3], or using a McLaurin series expansion of the trigonometric terms around a well-chosen guidance function [2]. Obviously, these existing methods do not allow for establishing the global convergence property of the solution.

C. Paper Description

The problem formulation is described in Section II. Section III describes the design of an asymptotically convergent kinematic control (Section III-A), extended to cope with vehicle dynamics (Section III-B) by resorting to backstepping and Lyapunov-based techniques (for details on this topic, please refer to [30]). The computation of such a control is shown in Section III-C and it provides a limitation of robot design. Robustness to uncertainty in the parameters of vehicle dynamics is addressed by incorporating a hybrid parameter-adaptation scheme (Section III-D). Section IV provides simulation results of the previously described controllers. Section V contains the conclusions and explanation of future work concerning this subject. It should be noted that this paper does not explicitly address the disturbance rejection problem (e.g., ocean current, waves effect, etc.).

II. Problem Formulation

This section introduces some basic notation, presents the kinematic equations of motion for an underactuated mobile robot, and formalizes the problem of driving the robot along a desired path, in the horizontal plane. The first part (Section II-A) shows the notations adopted throughout this paper. Section II-B describes the underactuated underwater robot, as depicted in Table II. Section II-C presents the kinematic equations of the system. Section II-D briefly presents the dynamic model of the robot. Finally, Section II-E states the problem of finding a controller that guarantees convergence to a desired path, taking into account the parametric uncertainties.

A. Notation

Throughout this paper, the following notations will be used.

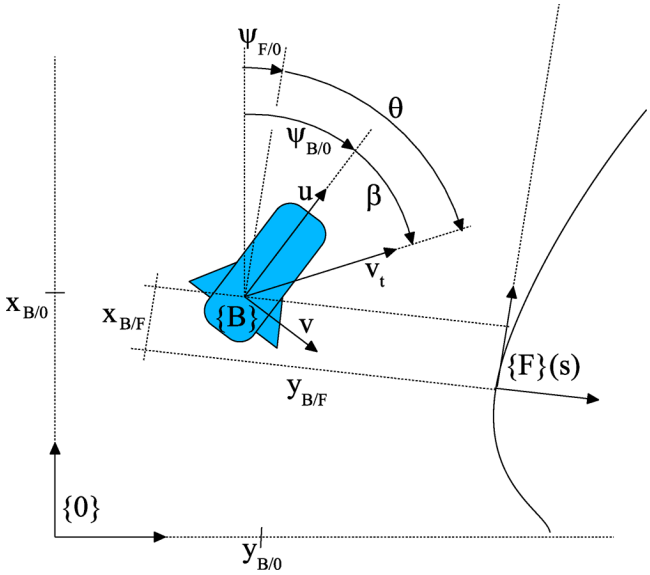

Fig. 1. Frame definition and description of the problem posed.

$\{A\}$ $:= \{x_A\ y_A\ z_A\}$. Reference frame with the origin in A. We let $\{0\}, \{F\}$, and $\{B\}$ be inertial, Serret–Frenet, and body axis frames, respectively.

$p_{A/B}$ $= [x_{A/B}\ y_{A/B}\ z_{A/B}]^T$. Position of the frame $\{A\}$ in relation to $\{B\}$. Note that $\dot{p}^C_{A/B} = [\dot{x}^C_{A/B}\ \dot{y}^C_{A/B}\ \dot{z}^C_{A/B}]^T$ represents the velocity of the frame $\{A\}$ in relation to $\{B\}$ expressed in $\{C\}$.

$\Psi_{A/B}$ Orientation of $\{A\}$ in relation to $\{B\}$, and $\dot{\Psi}_{A/B}$ the angular velocity of $\{A\}$ in relation to $\{B\}$.

R^B_A Rotational matrix from $\{A\}$ to $\{B\}$.

Note that because the study takes place in the horizontal plane, $z_{A/B} =$ constant and $\dot{z}^C_{A/B} = 0, \forall (A, B, C)$.

B. Vehicle Description

The vehicle has two identical rear thrusters, mounted symmetrically with respect to its longitudinal axis of symmetry. Each thruster generates a control force F_i, $i = 1, 2$, and a torque that we consider negligible. The common action mode of the thrusters results in a forward force F, and their differential action mode generates a torque Γ. $[\Gamma F]^T$ defines the dynamic system input.

We assume that the vehicle is neutrally buoyant and that its metacenter coincides with the origin of $\{B\}$. $p_{B/0}$ specifies the absolute position of the origin of $\{B\}$ in $\{0\}$, and $\Psi_{B/0}$ is the parameter that represents the orientation of $\{B\}$ with respect to $\{0\}$, the yaw angle. $\dot{p}^B_{B/0} = [u\ v\ 0]^T$ denotes the absolute velocity of $\{B\}$ with respect to $\{0\}$, expressed in the body frame. u and v are the longitudinal (surge) and transverse (sway or sideslip) velocities, respectively. $\dot{\Psi}_{B/0} = r$ represents the heading velocity (Fig. 1). We also define the sideslip angle as

$$\beta = \arctan(v/u). \tag{1}$$

Note that the well poseness of this expression requires the following assumption:

$$|u| + |v| \neq 0 \Leftrightarrow v_t^2 = u^2 + v^2 \neq 0 \qquad \forall t$$

where v_t is the AUV's total velocity. Note that the control of an AUV system implies considering a permanent positive velocity, therefore the previous condition is covered by the following:

$$v_t > 0 \qquad \forall t. \tag{2}$$

C. Kinematic Model of the Robot

The kinematic model relates the inertial velocity expressed in the body frame $\{B\}$ with the one expressed in the inertial frame $\{0\}$, through the equation $\dot{p}^0_{B/0} = R^0_B . \dot{p}^B_{B/0}$. Extracting the meaningful relations yields

$$\begin{aligned} \dot{x}^0_{B/0} &= u\cos(\Psi_{B/0}) - v\sin(\Psi_{B/0}) \\ \dot{y}^0_{B/0} &= u\sin(\Psi_{B/0}) + v\cos(\Psi_{B/0}) \\ \dot{\Psi}_{B/0} &= r. \end{aligned} \tag{3}$$

Note that $[u\ r]^T$ defines the kinematic system inputs.

D. Dynamic Model of the Robot

The dynamic model of the chosen robot is the classical one described in (4). A complete model of the Infante AUV, developed at the DSOR***[AU: Please define DSOR]***, is described in [36]

$$\begin{aligned} F &= m_u \dot{u} + d_u \\ 0 &= m_v \dot{v} + m_{ur} ur + d_v \\ \Gamma &= m_r \dot{r} + d_r \end{aligned} \tag{4}$$

with

$$\begin{aligned} m_u &= m - X_{\dot{u}}, \quad & d_u &= -X_{uu}u^2 r - X_{vv}v^2 \\ m_v &= m - Y_{\dot{v}}, \quad & d_v &= -Y_v uv - Y_{v|v|}v|v| \\ m_r &= I_z - N_{\dot{r}}, \quad & d_r &= -N_v uv - N_{v|v|}v|v| - N_r ur \\ m_{ur} &= m - Y_r \end{aligned}$$

where m denotes the system mass, I_z is the moment of inertia with respect to the z-axis, and $X_{..}$, $Y_{..}$, and $N_{..}$ are the hydrodynamic derivatives of the system. For more information on the modeling of the Infante vehicle, please refer to [36]. Note that $[F\Gamma]^T$ defines the dynamic system inputs.

E. Problem Formulation

1) Side-Slipping Vehicle Control: The laws of mechanics show that the trajectory of a moving object is fully related to the amplitude and the orientation of its total velocity. These variables must be driven to a desired value to control the trajectory. The control strategy depends on the type of actuation mounted. From the actuation point of view, there exists a visible similarity between the underactuated underwater robot described in Section II-D and the classic nonholonomic wheeled unicycle-type robot. The main difference is that the nonholonomic constraint, active in the wheeled robot, is relaxed in the underactuated system. The direct consequence is that the total

velocity of a unicycle-type robot is permanently equal to its forward velocity u, while the total velocity of an underactuated vehicle results from both surge and sway components u and v [see (2)].

The path-following problem is solved for the unicycle-type robot by designing a control that drives the vehicle onto the path and then insures that the orientation of the forward velocity u stays tangent to the path. In the case of an underactuated vehicle, this is no longer valid. The transverse component of the velocity implies that the robot is not aligned with its total velocity, so while the unicycle case is solved by controlling the forward velocity u, the underactuated case requires the control of the total velocity v_t defined in (2). Designing a controller for a sideslipping vehicle implies driving the amplitude and the orientation of the total velocity to desired values, defined with respect to the path that the robot must reach and follow. The related variables are $||v_t||$ and $\theta = \beta + \Psi_{B/F}$. This implies a design limitation on a submarine robot controlled in this way, which is shown in Section III-C. It is because the kinematic controller involves a computation of $\dot{\beta}$, therefore a computation of $\dot{u}$ and $\dot{v}$, the longitudinal and transverse accelerations of the robot. Relying on the dynamic model injects dynamic parameters at the kinematic level. The backstepping process, used to design the dynamic control from the kinematic ***[AU: Kinematic what?]***, reveals the necessary computation of $\ddot{\beta}$, hence $\ddot{u}$ and $\ddot{v}$, the transverse and longitudinal system jerks. Once again, this is achieved using the dynamic model, and it implicitly implies deriving longitudinal and transverse acceleration expression from the dynamical model. This emphasizes the limit of the hypothesis made during the drawing up of the dynamical model, especially the neglected high-order terms. On the other hand, a hybrid adaptation scheme can be designed (Section III-D) that relaxes the necessity for high accuracy in the estimation of the constant model parameters.

2) Path Following: To derive a controller for a path-following problem, the equations of the system must be derived relative to a given path, and the goal of the controller is to drive the robot to reach and follow the path, without time constraint. The parameterization of the problem is illustrated in Fig. 1. Referring to Fig. 1, given any point F on the path, a controller that drives θ to 0, as $x_{B/F}$ and $y_{B/F}$ go to 0, solves the path-following problem. The difference in the strategies that can be adopted concerns the definition of point F. In [33], point F is defined as the closest point on the path with respect to the current position of the robot. In this case, the line (BF) is always perpendicular to the path tangent on F. Thus, the parameterization of the problem is simpler, convergence is guaranteed when $||BF||$, and θ are driven to 0. However, this method implies a singularity when point B is located at the center of the path curvature, at point F (θ is undefined). Locate point F by its curvilinear abscissa s_F, and name $c_c(s_F)$ the path curvature at this point. Then, the singularity occurs when $||BF|| = 1/c_c(s_F)$. In addition, the analysis in [34] shows that global convergence is guaranteed only if $||BF|| < 1/c_c^{\max}$ for all locations of F, and for $c_c^{\max}$ defining the maximum curvature encountered on the path. This is a very restrictive hypothesis that implies a considerable limitation on the initial condition $||BF||_{t=0} < 1/c_c^{\max}$ and a poor disturbance rejection capability. Another solution consists in defining point F as a virtual moving target that describes the path. The movement control of this target introduces a supplementary virtual state into the system, but transforms the previous constraint to $||BF||_{t=0} \neq [c_c(s|_{t=0})]^{-1}$. The behavior of the virtual target (captured in the expression of $\dot{s}_F$) is chosen according to the derivation of Lyapunov functions in the backstepping process, and results in a very cooperative target that quickly converges to the closest point on the path. Expressed in the Serret–Frenet frame $\{F\}$, the kinematic equations of the problem are rewritten as

$$\begin{aligned} \dot{x}_{B/F} &= -\dot{s}_F\left(1 - c_c(s_F)y_{B/F}\right) + v_t\cos\theta \\ \dot{y}_{B/F} &= -c_c(s_F)\dot{s}_F x_{B/F} + v_t\sin\theta \\ \dot{\theta} &= r + \dot{\beta} - c_c(s_F)\dot{s}_F. \end{aligned} \tag{5}$$

3) Mathematical Formulation: Equipped with this formalism ***[AU: Formulation?]***, we can now state the kinematic control problem $\mathbf{C_1}$ that is addressed in Section III-A.

> $\mathbf{C_1}$: Given the robot kinematic model (3), the robot dynamic model (4), and a set of available measurements coming from robot sensors, compute $U_{kin} = [u(.)\ r(.)\ \dot{s_F}]^T$, so that $\theta, x_{B/F}$, and $y_{B/F}$ converge to 0 as t goes to ∞.

This problem will be extended in Section III-B to explicitly deal with vehicle dynamics. The dynamic control problem $\mathbf{C_2}$ is stated as follows.

> $\mathbf{C_2}$: Given the robot kinematic model (3), the robot dynamic model (4), and a set of available measurements coming from robot sensors, compute $U_{\text{dyn}} = [F(.)\ \Gamma(.)\ \dot{s_F}]^T$, so that $\theta, x_{B/F}$, and $y_{B/F}$ converge to 0 as t goes to ∞.

Note that the validity of statement $\mathbf{C_2}$ implies that there is no external disturbance, sensor noise, or unmodeled dynamics, and a perfect knowledge of the system parameters. Consider that there is no external disturbances, sensor noise, or unmodeled dynamics, but that the parameters are not perfectly known. Section III-C describes another version of the dynamic controller that guarantees robustness against parameter uncertainty and solves problem $\mathbf{C_3}$, stated as follows.

> $\mathbf{C_3}$: Given the robot kinematic model (3), the robot dynamic model (4), a set of available measurements coming from robot sensors, and a set of reasonable estimation of the nine parameters of the dynamic model, compute $U_{\text{dyn}}^{Rbst} = [F(.)\ \Gamma(.)\ \dot{s_F}\ \dot{p_i}]^T$, so that $\theta, x_{B/F}$, and $y_{B/F}$ converge to 0 as t goes to ∞.

The effects of external disturbance, sensor noise, or unmodeled dynamics are not treated in this paper. The solution consists in proving the boundedness of the system output in the presence of bounded external disturbance and unmodeled dynamics effect, and extracting from the expression of the bounded system output the meaningful information related to the performance of the controlled system.

A proposed solution for problems $\mathbf{C_i}$ $(i = 1, 2, 3)$ is described in the following section.

III. Controller Design

This section describes the solutions to problems $\mathbf{C_1}$, $\mathbf{C_2}$, and $\mathbf{C_3}$, stated in the previous section. In the following, we will extensively use a corollary of Barbalat's lemma (CBL), and LaSalle's theorem, stated as follows.

Barbalat's Lemma: If $f(t)$ is a double differentiable function such that $f(t)$ is finite as t goes to ∞, and such that $\dot{f}(t)$ is uniformly continuous, then $\dot{f}(t)$ tends to 0 as t tends to ∞.

Uniform Continuity Sufficient Condition: $\dot{f}(t)$ is uniformly continuous if $\ddot{f}(t)$ exists and is bounded.

Corollary of Barbalat's Lemma: If $f(t)$ is a double differentiable function such that $f(t)$ is finite as t goes to ∞, and such that $\ddot{f}(t)$ exists and is bounded, then $\dot{f}(t)$ tends to 0 as t tends to ∞.

LaSalle's Theorem: Let Ω be a positively invariant set of the system described in (3) and (4). Suppose that every solution starting in Ω converges to a set $E \subset \Omega$ and let M be the largest invariant set contained in E. Then, every bounded solution starting in Ω converges to M as t tends to ∞.

For details of Barbalat's lemma and its application, please refer to [37]. For demonstration and application of LaSalle's theorem, please refer to [35] and [29]. Note that the application of LaSalle's theorem is restricted to autonomous systems. In our situation, the fact that the desired forward velocity is constant allows us to consider our system as autonomous.

A. Kinematic Controller

With the formalism developed previously, we may now state the following theorem.

Proposition 1: Consider the robot models (3) and (4) and let a desired approach angle be defined by

$$\delta(y_{B/F}) = -\theta_a \frac{e^{2k_\delta y_{B/F}} - 1}{e^{2k_\delta y_{B/F}} + 1} \tag{6}$$

where k_δ is a positive gain and $0 < \theta_a < \pi/2$. Further, assume that measurements of $[u\ v]^T$ are available from robot sensors and that a parameterization of the path is available such that given s_F, the curvilinear abscissa of a point on the path, the variables $\theta, x_{B/F}, y_{B/F}$, and $c_c(s_F)$ are well defined and computable. Then, the control law

$$U_{kin} = \begin{cases} r = \dot{\delta} - \dot{\beta} - K_1(\theta - \delta) + c_c(s_F)\dot{s}_F \\ \dot{s_F} = \cos\theta v_t + K_2 x_{B/F} \end{cases} \tag{7}$$

solves problem $\mathbf{C_1}$, with K_1, K_2, and k_δ three arbitrary positive gains, the assumption that $v_t > 0, \forall t$, and given the initial relative position $[\theta, x_{B/F}, y_{B/F}]|_{t=0}$.

Proof: The proof is structured in three parts. First, we show that the system asymptotically follows the reference angle δ. Then, we show that the reference asymptotically drives the robot onto the path. Finally, we use the LaSalle invariance principle to concatenate the two previous convergence properties.

Consider the following Lyapunov function $V_1 = (1/2)(\theta - \delta)^2$. It is straightforward to show that the choice of the control

$$r = \dot{\delta} - \dot{\beta} - K_1(\theta - \delta) + c_c(s_F)\dot{s}_F$$

yields $\dot{V}_1 = -K_1(\theta - \delta)^2 \leq 0$. That is, V_1 is a positive and monotonically decreasing function up to a well-defined limit

$$\lim_{t\to\infty} V_1 = l_1. \tag{8}$$

Simple derivation shows that $\ddot{V}_1 = 2K_1^2(\theta - \delta)^2$, which is bounded since (8). Then, using the CBL, we conclude that $\lim_{t\to\infty} \dot{V}_1 = 0$. That is

$$\lim_{t\to\infty} \theta = \delta|_{t\to\infty}. \tag{9}$$

The system asymptotically follows the reference $\delta(y_{B/F})$ defined in (6), so the trajectories of the system will asymptotically reach the invariant set E defined as

$$E := \left((x_{B/F}, y_{B/F}) \in \Re^2, \dot{V}_1 = 0\right). \tag{10}$$

For the sake of clarity, define $x = x_{B/F}$, $y = y_{B/F}$, and $s = s_F$, and recall (5). Study the trajectories of the system onto the invariant set E. Consider the Lyapunov candidate $V_E = (1/2)(x^2 + y^2), \forall (x, y) \in E$. It is straightforward to show that the choice

$$\dot{s} = v_t \cos\theta + K_2 x \tag{11}$$

leads to

$$\dot{V}_E = y v_t \sin\delta - K_2 x^2 < 0 \qquad \forall ((x, y) \neq 0) \in E \tag{12}$$

since onto the set ***[AU: Delete "onto"? It is unclear here. Please rewrite.]*** $E : \theta = \delta$, $sign(\delta) = -sign(y)$, $\delta \in [-\theta_a\ \theta_a]$, $0 < \theta_a \leq \pi/2$, and using the assumption $\lim_{t\to\infty} v_t > 0$, covered by the necessary assumption for the definition of (2). Therefore, V_E is finite.

Moreover, it is straightforward to show that $\ddot{V}_E$ is bounded, and we use the CBL to prove that $\lim_{t\to\infty} \dot{V}_E = 0$, which implies $\lim_{t\to\infty} y = 0$ and $\lim_{t\to\infty} x = 0$, since (12). Hence, $(x, y) = (0, 0)$ is the unique stable point of E, and every trajectory of the system starting in E asymptotically converges to the origin.

We now use LaSalle's invariance principle. Let $\Omega = \Re^2$. The first part of the proof showed that every solution starting in Ω asymptotically converges to E. The second step showed that the largest invariant set of E is $M = [(x, y) = 0^2]$, so every bounded solution starting in Ω converges to 0 as t tends to ∞. ■

B. Dynamic Controller

The development of the dynamic control is based on the previous result, considering the kinematic control as a reference, called r_d, for the dynamic control

$$\begin{cases} r_d = \dot{\delta} - K_1(\theta - \delta) - \dot{\beta} + c_c(s)\dot{s} \\ \dot{s} = \cos\theta v_t + K_2 x_{B/F}. \end{cases} \tag{13}$$

Let $\epsilon_r = r - r_d$ and consider the Lyapunov candidate V_2

$$V_2 = K_5 V_1 + \frac{1}{2}\epsilon_r^2 + \frac{1}{2}(u - u_d)^2 \tag{14}$$

with K_5 being a positive gain. Simple computations show that

$$\begin{cases} \dot{r} = \dot{r_d} - K_3(r - r_d) - K_5(\theta - \delta) \\ \dot{u} = \dot{u_d} - K_4(u - u_d) \end{cases} \tag{15}$$

where $\dot{u}_d = 0$ in our study case. Recall that $\dot{\theta} = r - c_c\dot{s} + \dot{\beta}$, then

$$\dot{V}_2 = -K_1K_5(\theta - \delta)^2 - K_3(r - r_d)^2 - K_4(u - u_d)^2 \leq 0.$$

Note that this condition is more restrictive than necessary. The condition that the desired velocity profile is invariant is enough. It is now straightforward to compute the control inputs F and Γ by solving the dynamics (4) to obtain

$$U_{\text{dyn}} = \begin{cases} \Gamma = m_r\Big(\ddot{\delta} - \ddot{\beta} - (K_1 + K_3)(\dot{\theta} - \dot{\delta}) - (K_5 + K_1K_3) \\ \qquad \times(\theta - \delta) + c_c\ddot{s} + \dfrac{\partial c_c}{\partial s}\dot{s}^2\Big) + d_r \\ F = m_u\left(\dot{u_d} - K_4(u - u_d)\right) + d_u. \end{cases} \tag{16}$$

We can now state Proposition 2 that solves problem $\mathbf{C_2}$.

Proposition 2: Consider the robot models (3) and (4) and the desired approach angle defined in (6), where k_δ is a positive gain and $0 < \theta_a < \pi/2$. Further, assume that measurements of $[u\ v\ r]^T$ are available from robot sensors and that a parameterization of the path is available such that, given s, the curvilinear abscissa of a point on the path, the variables $\theta, x_{B/F}, y_{B/F}, c_c, (\partial c_c/\partial s)$ are well defined and computable. Define u_d as the desired forward velocity. Then, control law (16) and expression (7), with K_1, K_2, K_3, K_4, and K_5 positive gains, the assumption that $v_t > 0, \forall t$, and given the initial relative position $[\theta, x_{B/F}, y_{B/F}]|_{t=0}$, solve problem $\mathbf{C_2}$.

Proof: Considering the V_2 (14) Lypaunov function, and using the CBL, as previously, it is straightforward to show that

$$\begin{aligned} &\lim_{t\to\infty}\theta = \delta|_{t\to\infty} \\ &\lim_{t\to\infty}\dot{\theta} = \dot{\delta}|_{t\to\infty} \\ &\lim_{t\to\infty}u = u_d. \end{aligned}$$

Thus, the trajectories of the system will reach the invariant set E

$$E := \Big((x_{B/F}, y_{B/F}) \in \Re^2, \dot{V}_2 = 0\Big).$$

Using the same argument as that used in the previous proof (kinematic case) and the assumption that $v_t > 0$ proves the convergence of the system to the path. ■

C. Computation of the Control

The previous control U_{dyn} guarantees the asymptotic convergence to the path. Nevertheless, the terms appearing in (15) are not trivially computable. In particular, the computation of $\ddot{\beta}$ refers to the evaluation of jerks $\dddot{u}$ and $\dddot{v}$ through

$$\ddot{\beta} = \frac{1}{v_t^2}(\dddot{v}u - \dddot{u}v) - 2\frac{\dot{v}_t}{v_t}\dot{\beta}. \tag{17}$$

Because it is not realistic to have any measurement of these quantities, the only solution is to rely on a derivation of the dynamic model such that

$$\begin{cases} \dddot{u} = \dfrac{1}{m_u}(\ddot{F} - \ddot{d}_u) \\ \dddot{v} = \dfrac{1}{m_v}(-m_{ur}\ddot{u}r - m_{ur}u\ddot{r} - \ddot{d}_v). \end{cases} \tag{18}$$

This emphasizes the assumption made regarding the neglected dynamics of the system. Then, $\dot{r}$ is rewritten

$$\dot{r} = \frac{f_{\dot{r}_d} - K_3(r - r_d) - K_5(\theta - \delta)}{1 - \dfrac{m_{ur}}{m_v}(\cos\beta)^2}$$

where

$$\begin{aligned} f_{\dot{r}_d} = \dddot{\delta} - K_1(\ddot{\theta} - \ddot{\delta}) + c_c\dddot{s} + g_c\ddot{s} + \frac{\dddot{u}v}{v_t^2} \\ + \frac{2\dot{v}_t\ddot{\beta}}{v_t} + \frac{u}{v_t^2}\left(\frac{m_{ur}}{m_v}\ddot{u}r + \frac{\ddot{d}_v}{m_v}\right). \end{aligned}$$

Then, the control is computed as

$$\Gamma = m_r\dot{r} + d_r.$$

For this expression to be well posed, it must be derived from the robot design parameter

$$\frac{m_{ur}}{m_v} = \frac{m - Y_r}{m - Y_{\dot{v}}}.$$

Analyzing the signs of the hydrodynamic parameters as in [1], we know the following:

- $Y_{\dot{v}}$ is always negative;
- Y_r is positive if stern dominates;
- Y_r is negative if bow dominates.

Thus, in the case of a stern dominant vehicle, the control computation is well posed. For a bow dominant vehicle, the sign of $m - Y_r$ should be taken into account.

D. Robust Control

This section addresses the question of robustness to parameter uncertainties. The previous dynamic control is modified to relax the constraint of having a precise estimation of the dynamic parameters by resorting to backstepping Lyapunov-based techniques.

Recall that the design of the kinematic reference requires an estimation of surge and sway acceleration, relying on the dynamic model, so the errors due to parameters misestimation should explicitly be taken into account in the elaboration of the kinematic reference.

1) Kinematic Reference: In Section III-A, we designed a kinematic reference (13) that includes the computation of $\dot{\beta}$, which can be rewritten as

$$\dot{\beta} = -\sum_{i=1}^{2} q_i g_i - q_3 g_3 r + \dot{u}\frac{v}{v_t^2}.$$

The expression of functions g_i and parameters q_i is displayed in the Appendix. Because r explicitly appears in the previous relation, a proper expression of the kinematic reference is extracted by solving (13) for r, and naming r as r_d, the kinematic reference

$$r_d = \frac{f_r + \sum_{i=1}^{2} q_i g_i - \dot{u}\dfrac{v}{v_t^2}}{1 - q_3 g_3} \tag{19}$$

with $f_r = \dot{\delta} - K_1(\theta - \delta) + c_c(s)\dot{s}$. It should be explicitly established that the resulting expression is well posed in the function of the value of q_3, as mentioned for the dynamic case in Section III-B. This question will be addressed at the dynamic level.

The optimal value for r_d is computed with the real value of parameters q_i^{Re} and a perfect estimation of the forward acceleration $\dot{u}^{\mathrm{Opt}}$. Then, the use of estimated values q_i of the dynamic parameters induces an error such that

$$\Delta r = \frac{\sum_{i=1}^{2} \Delta q_i g_i - \Delta\dot{u}\dfrac{v}{v_t^2} + \Delta q_3 g_3 r}{1 - q_3^{\mathrm{Re}} g_3}$$

with $\Delta q_i = q_i^{\mathrm{Re}} - q_i$ $(i = 1,2,3)$, $\Delta\dot{u} = \dot{u}^{\mathrm{Opt}} - \dot{u}$, and $\Delta r = r^{\mathrm{Opt}} - r$.

Consider the Lyapunov candidate $V_1 = (1/2)(\theta - \delta)^2$. The misestimation of the parameters induces a nonnegative derivative $\dot{V}_1$

$$\dot{V}_1 = -K_1(\theta - \delta)^2 + (\theta - \delta)\Delta r.$$

Because $\dot{V}_1$ is not negative definite, we cannot conclude any convergence property, since the effects of the parameter misestimation still appear in the Lyapunov candidate. Nevertheless, these effects will be canceled at the dynamic level, and asymptotic convergence will be guaranteed. Consider the suboptimal kinematic control (19) as a reference to drive the dynamic controller

$$\tilde{r}_d = \frac{f_r + \sum_{i=1}^{2} q_i g_i - \dot{u}\dfrac{v}{v_t^2}}{1 - q_3 g_3} \tag{20}$$

given q_i, an estimation of q_i^{Re} $(i = 1,2,3)$.

2) Robust Dynamic Control: To deal with robustness to parameter uncertainty, it is necessary to expand the dynamic control expression (16) to make the parameters explicitly appear in the equations, and study the incidence of their misestimation. Considering the previous suboptimal kinematic control as a reference $\tilde{r}_d$ (20), we derive the dynamic control as in Section III-B, explicitly extracting the dynamic parameters

$$\begin{aligned}\tilde{\Gamma} = m_r\left(\dot{\tilde{r}}_d - K_3(r - \tilde{r}_d) - K_5(\theta - \delta)\right)\\ - m_{uv}uv - N_r r - N_{r|r|}r|r|\end{aligned}$$

with

$$\dot{\tilde{r}}_d = R_0^{\dot{r}_d} + \dot{v}R_{\dot{v}}^{\dot{r}_d} + \dot{u}R_{\dot{u}}^{\dot{r}_d} + \ddot{u}R_{\ddot{u}}^{\dot{r}_d} + \dot{u}^2 R_{\dot{u}^2}^{\dot{r}_d} + \dot{u}\dot{v}R_{\dot{u}\dot{v}}^{\dot{r}_d}$$

where $R_0^{\dot{r}_d}, R_{\dot{v}}^{\dot{r}_d}, R_{\dot{u}}^{\dot{r}_d}, R_{\ddot{u}}^{\dot{r}_d}, R_{\dot{u}^2}^{\dot{r}_d}, R_{\dot{u}\dot{v}}^{\dot{r}_d}$ are computable functions dependent on the measurements, listed in the Appendix. Then, $\tilde{\Gamma}$ is rewritten as

$$\begin{aligned}\tilde{\Gamma} = {} & m_r\left(R_0^{\dot{r}_d} - K_3(r - \tilde{r}_d) - K_5(\theta - \delta)\right)\\ & - m_{uv}uv - N_r r - N_{r|r|}r|r| + m_r\dot{v}R_{\dot{v}}^{\dot{r}_d}\\ & + m_r\left(\dot{u}R_{\dot{u}}^{\dot{r}_d} + \ddot{u}R_{\ddot{u}}^{\dot{r}_d} + \dot{u}^2 R_{\dot{u}^2}^{\dot{r}_d} + \dot{u}\dot{v}R_{\dot{u}\dot{v}}^{\dot{r}_d}\right).\end{aligned} \tag{21}$$

Consider now the following version of the control $\tilde{\tilde{\Gamma}}$:

$$\begin{aligned}\tilde{\tilde{\Gamma}} = {} & m_r(R_0^{\dot{r}_d} - K_3(r - \tilde{r}_d) - K_5(\theta - \delta))\\ & - m_{uv}uv - N_r r - N_{r|r|}r|r| + m_r\dot{v}R_{\dot{v}}^{\dot{r}_d}.\end{aligned} \tag{22}$$

Hence, a misestimation of the robot parameters yields a computed control that differs from its optimal version by

$$\begin{aligned}\Delta\tilde{\tilde{\Gamma}} = {} & \Delta[m_r]\left(R_0^{\dot{r}_d} - K_3(r - \tilde{r}_d) - K_5(\theta - \delta)\right)\\ & - \Delta[m_{uv}]uv - \Delta[N_r]r - \Delta[N_{r|r|}]r|r| + \Delta[m_r\dot{v}]R_{\dot{v}}^{\dot{r}_d}\\ & + m_r^{\mathrm{Re}}\dot{u}^{\mathrm{Opt}}\dot{v}^{\mathrm{Opt}}R_{\dot{u}\dot{v}}^{\dot{r}_d}\\ & + m_r^{\mathrm{Re}}\left(\dot{u}^{\mathrm{Opt}}R_{\dot{u}}^{\dot{r}_d} + \ddot{u}^{\mathrm{Opt}}R_{\ddot{u}}^{\dot{r}_d} + (\dot{u}^{\mathrm{Opt}})^2 R_{\dot{u}^2}^{\dot{r}_d}\right)\end{aligned}$$

with $\Delta[m_r\dot{v}] = m_r^{\mathrm{Re}}\dot{v}^{\mathrm{Opt}} - m_r\dot{v}$, and so on. Using the expression of $\dot{v}$, extracted form (4), $\Delta\tilde{\tilde{\Gamma}}$ is rewritten as

$$\Delta\tilde{\tilde{\Gamma}} = \sum_{i=1}^{7}\Delta p_i f_i + \Phi(.)$$

where $\Phi(.) = m_r^{\mathrm{Re}}\dot{u}^{\mathrm{Opt}}\dot{v}^{\mathrm{Opt}}R_{\dot{u}\dot{v}}^{\dot{r}_d} + m_r^{\mathrm{Re}}(\dot{u}^{\mathrm{Opt}}R_{\dot{u}}^{\dot{r}_d} + \ddot{u}^{\mathrm{Opt}}R_{\ddot{u}}^{\dot{r}_d} + (\dot{u}^{\mathrm{Opt}})^2 R_{\dot{u}^2}^{\dot{r}_d})$. The parameters p_i and the functions f_i are listed in the Appendix.

Consider the following Lyapunov candidate that captures the system's property of convergence to the suboptimal reference $\tilde{r}_d$:

$$V_6 = \frac{1}{2}(r - \tilde{r}_d)^2 + \frac{1}{2}\sum_{i=1}^{7}\frac{(\Delta p_i)^2}{\lambda_i^p}$$

and, with control (21) and parameter adaptation scheme

$$\dot{p}_i = -\lambda_i^p(r - \tilde{r}_d)f_i, \qquad i = 1\ldots 7 \tag{23}$$

yields the following derivative:

$$\dot{V}_6 = -K_3(r - \tilde{r}_d)^2 + (r - \tilde{r}_d)\Phi(.).$$

Consider now the forward control, and expand (16)

$$F = \sum_{i=1}^{4} d_i l_i. \tag{24}$$

The parameters d_i and the functions l_i are listed in the Appendix. The misestimation $\Delta d_i = d_i^{\mathrm{Re}} - d_i$, for $i = 1,2,3,4$,

induces a computed forward control different from the optimal one such that

$$\Delta F = F^{\mathrm{Opt}} - F = \sum_{i=1}^{4} \Delta d_i l_i.$$

Then, considering the following Lyapunov candidate:

$$V_5 = \frac{1}{2}(u-u_d)^2 + \frac{1}{2}\sum_{i=1}^{4}\frac{\Delta d_i l_i}{\lambda_i^d}$$

with control (24) and the following parameter adaptation scheme:

$$\dot{d}_i = -\lambda_i^d (u-u_d) l_i, \qquad i = 1\ldots 4 \tag{25}$$

leads to a negative–definite derivative

$$\dot{V}_5 = -K_5(u-u_d)^2 \leq 0.$$

Then, noting that $\ddot{V}_5$ is bounded, the use of the CBL proves the asymptotic convergence of u to u_d. Hence, $\dot{u}$ and $\ddot{u}$ vanish with time

$$\lim_{t\to\infty} \dot{u} = 0$$
$$\lim_{t\to\infty} \ddot{u} = 0.$$

The previous argument implies that the system will asymptotically reach the invariant set

$$\Omega^{\dot{u}} = [x, y, \theta, u, v, r, s | \dot{u} = 0, \ddot{u} = 0]. \tag{26}$$

Studying the system trajectories onto the $\Omega^{\dot{u}}$ set, we notice that

$$\Phi(.)|_{\Omega^{\dot{u}}} = 0$$

hence

$$\dot{V}_6|_{\Omega^{\dot{u}}} = -K_3(r-\tilde{r}_d)^2 \leq 0.$$

Noting that $\ddot{V}_6$ is bounded, and using the invariance principle, the previous arguments imply

$$\lim_{t\to\infty} r = \tilde{r}_d.$$

Then, the system will asymptotically reach the invariant set $\Omega^{\tilde{r}_d} \subset \Omega^{\dot{u}}$ defined as

$$\Omega^{\tilde{r}_d} = [x, y, \theta, u, v, r, s | r = \tilde{r}_d]. \tag{27}$$

The system trajectories onto this set are described by the $V_1|_{\Omega^{\tilde{r}_d}}$ Lyapunov candidate. In this set, the derivative is written as

$$\dot{V}_1|_{\Omega^{\tilde{r}_d}} = \frac{(\theta-\delta)}{1-q_3^{\mathrm{Re}} g_3}\left(\sum_{i=1}^{2}\Delta q_i g_i + \Delta q_3 g_3 r\right) - K_1(\theta-\delta)^2.$$

The effects of the misestimation of parameter q_i are still present, and we do not consider the previously used solution of adapting its estimation since the knowledge of q_3^{Re} is required to design a classic adaptive scheme.

The proposed solution consists in relying on switching control system theory to guarantee that $\dot{V}_1$ is negative definite. For more information on switching control systems, please refer to [27] and [32]. To insure asymptotic convergence, one should insure that

$$\frac{(\theta-\delta)}{1-q_3^{\mathrm{Re}} g_3}\left(\sum_{i=1}^{2}\Delta q_i g_i + \Delta q_3 g_3 r\right) \leq 0 \qquad \forall t.$$

This can be done by choosing two different values q_i^{up} and q_i^{down}, guaranteed to overestimate and underestimate the real value q_i^{Re} ($\Delta q_i^{\mathrm{up}} > 0$ and $\Delta q_i^{\mathrm{down}} < 0$), and use them such that

$$q_i = \begin{cases} q_i^{\mathrm{up}}, & \text{if } (\theta-\delta) g_i < 0 \\ q_i^{\mathrm{down}}, & \text{if } (\theta-\delta) g_i > 0 \end{cases}$$
$$q_3 = \begin{cases} q_3^{\mathrm{up}}, & \text{if } (\theta-\delta) r < 0 \\ q_3^{\mathrm{down}}, & \text{if } (\theta-\delta) r > 0 \end{cases} \tag{28}$$

using the facts that $g_3 > 0$ and $(1 - q_3 g_3) > 0, \forall t$. Then, using (28) switching conditions, we conclude that $\dot{V}_1|_{\Omega^{\dot{u}}} < 0$.

Because eight possible Lyapunov functions are negative definite, and the switching process does not affect the convergence [27], we can state that

$$\lim_{t\to\infty} \theta = \delta|_{t\to\infty}.$$

Using the same argument concerning the imbricated invariant set, it has been shown that the robot asymptotically converges to the path. We are now able to state Proposition 3 that solves problem $\mathbf{C_3}$.

Proposition 3: Consider the robot models (3) and (4) and the desired approach angle defined in (6), where k_δ is a positive gain and $0 < \theta_a < \pi/2$. Further, assume that measurements of $[u\ v\ r]^T$ are available from robot sensors and that a parameterization of the path is available such that, given s, the curvilinear abscissa of a point on the path, the variables $\theta, x_{B/F}, y_{B/F}, c_c, (\partial c_c/\partial s)$ are well defined and computable. Consider that a reasonable estimation of the model parameters $\tilde{m}_u, \tilde{m}_v, \tilde{m}_r, \tilde{m}_{uv}, \tilde{X}_u, \tilde{X}_{u|u|}, \tilde{Y}_v, \tilde{Y}_{v|v|}, \tilde{N}_r, \tilde{N}_{r|r|}$ was used to compute the 11 initial values p_i^0, d_j^0 $(i = 1\ldots 7, j = 1\ldots 4)$ as described in the tables of the Appendix, and q_k^{up} and q_k^{down} such that $q_k^{\mathrm{up}} > q_k^{\mathrm{Re}} > q_k^{\mathrm{down}}$, $(k = 1\ldots 3)$. Define u_d as the desired forward velocity. Then, the control law

$$U_{\mathrm{dyn}}^{\mathrm{Rbst}} = \begin{cases} \Gamma = \sum_{i=1}^{7} p_i f_i \\ F = \sum_{j=1}^{4} d_j l_j \end{cases} \tag{29}$$

with the kinematic reference

$$\tilde{r}_d = \frac{1}{1-q_3 g_3}\left(\dot{\delta} - K_1(\theta-\delta) + c_c(s)\dot{s} - (\dot{u}_d - K_5(u-u_d))\frac{v}{v_t^2} + \sum_{k=1}^{2} q_k g_k\right)$$
$$\dot{s} = v_t \cos\theta + K_2 x_{B/F}$$

the adaptation scheme (23), (25) and the switching scheme (28), with $\lambda_i^p, \lambda_j^d, K_1, K_2, K_3, K_4, K_5$ positive gains, the assumption that $v_t > 0, \forall t$, and given the initial relative position $[\theta, x_{B/F}, y_{B/F}]|_{t=0}$, solves problem $\mathbf{C_3}$.

TABLE I
PATH PARAMETERS

$a_0 = 0\, a_1 = 0.866\, a_2 = -0.02\, a_3 = 10^{-5}\, a_4 = 1.5.10^{-6}$
$b_0 = 0\, b_1 = 0.5\, b_2 = -5.10^{-4}\, b_3 = 10^{-5}\, b_4 = 10^{-7}$

Fig. 2. Infante AUV (IST) during its first sea trial.

Note that the evolution of the parameters is a function of the excitation of the problem. Analyzing the adaptation equations, it is easy to see that the adaptation stops when the reference errors $(r - r_d)$ and $(\theta - \delta)$ are equal to zero. This phenomenon is easily observed for linear systems when the path does not lead to sufficient excitation, and in this case, the estimated value of the parameters does not converge to the real value [31], [38].

Another solution, based on switching system theory, is imaginable. It consists in developing a switching scheme for all parameters, as for the q_i parameters. Further research on this topic is warranted.

IV. SIMULATION RESULTS

The aim of the simulation is to illustrate the efficiency of the previous controllers in driving an AUV onto a desired path. The path is characterized by a curvature c_c on a point F, parameterized by its curvilinear abscissa s. The objective is to regulate the distance to the path and the heading of the total velocity of the robot to zero relative to the given path. To test these controllers in a general case, we have chosen to consider the more complex path defined in Section IV-A.

A. Path Parameterization

The path is designed in Cartesian space (cf., Table I) and we assume to have a parameterization that allows the computation of the following items (given s):

- $\Psi_{F/0}(s)$: the global heading of the virtual target;
- $c_c(s)$: the path curvature at the target position;
- $\partial c_c(s)/\partial s$: the curvilinear derivative of the curvature at the target position;
- $x_{F/0}$ and $y_{F/0}$, the absolute location of the virtual target.

We have chosen a polynomial parameterization of the form

$$x_{F/0}(\mu) = \sum_{i=0}^{n} a_i \mu^i, \quad y_{F/0}(\mu) = \sum_{i=0}^{n} b_i \mu^i.$$

TABLE II
PARAMETERS OF THE SIMPLIFIED MODEL OF THE INFANTE AUV (IST) ***[AU: Please add space between unit and number; please change a period between units to a \cdot and please use regular font, not italics to present units]***

$m = 2234Kg$	$I_z = 2000N.m.s^2$
$X_{\dot{u}} = -142Kg.$	$Y_{\dot{v}} = -1715Kg.$
$N_{\dot{r}} = -1349N.m.s^2$	$X_u = 0Kg.m^{-1}$
$Y_v = -346Kg.m^{-1}$	$N_r = -1427N.m.s.$
$X_{u\|u\|} = -35Kg.m^{-1}$	$Y_v\|v\| = -667Kg.s^{-1}$
$N_r\|r\| = -310N.m.s.$	

TABLE III
DYNAMIC CONTROL PARAMETERS

$K_1 = 1$	$K_2 = 1$	$K_3 = 1$	$K_4 = 1$	$K_5 = 1$
$K_\delta = 1$	$\theta_a = \pi/4$	$u_d = 2$	$\dot{u}_d = 0$	$\ddot{u}_d = 0$

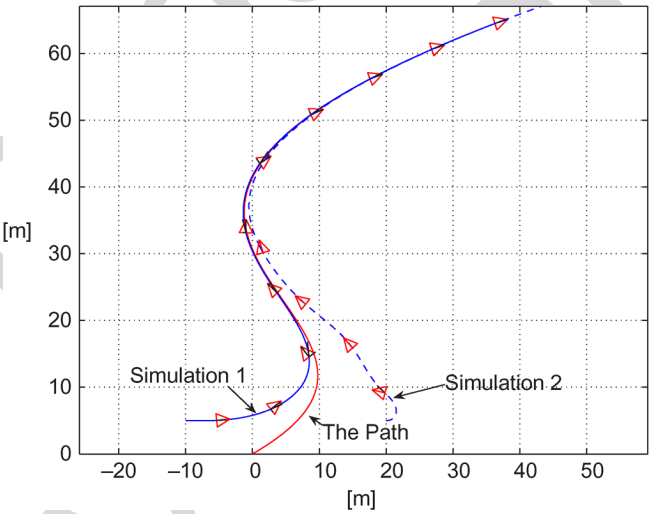

Fig. 3. System trajectories, when considering a perfect knowledge of the parameters (simulation 1: solid line; simulation 2: dashed line).

Assuming we have a precise estimation of function $\mu(s)$, and given s, we compute

$$\begin{aligned}
\Psi_{F/0}(s) &= \arctan \frac{(y_{F/0})'}{(x_{F/0})'} \\
c_c(s) &= \frac{\partial \Psi_{F/0}(s)}{\partial \mu} \frac{d\mu}{ds} \\
\frac{\partial c_c(s)}{\partial s} &= \frac{\partial c_c(s)}{\partial \mu} \frac{d\mu}{ds} \\
x_{F/0}(\mu(s)) \quad ; & \quad y_{F/0}(\mu(s)) \\
(x_{F/0})' = \frac{dx_{F/0}}{d\mu} \quad ; & \quad (y_{F/0})' = \frac{dy_{F/0}}{d\mu}.
\end{aligned}$$

The estimation of function $\mu(s)$ is achieved by integration of

$$\frac{d\mu}{ds} = \frac{1}{\sqrt{\left[(x_{F/0})'\right]^2 + \left[(y_{F/0})'\right]^2}}.$$

The model of the robot is a simplified version of Infante [36], the AUV developed at the DSOR (Fig. 2), given in Table II.

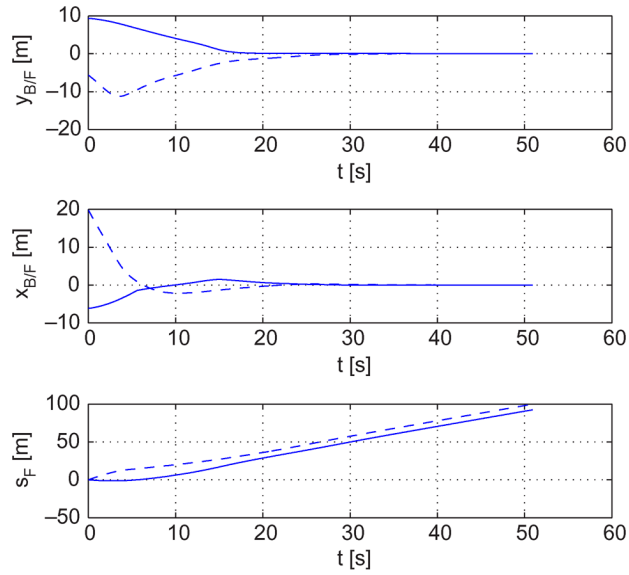

Fig. 4. Relative distance robot/rabit evolution, when considering a perfect knowledge of the parameters (simulation 1: solid line; simulation 2: dashed line).

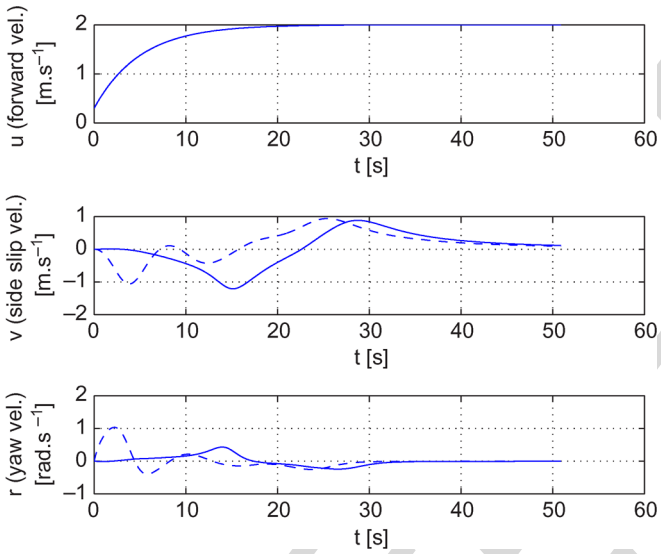

Fig. 5. System velocities evolution, when considering a perfect knowledge of the parameters (simulation 1: solid line; simulation 2: dashed line).

B. Dynamic Controller

The simulations are carried out using the robot parameters of Table II, the control parameters of Table III, and the path parameters of Table I.

The simulation results are displayed in Figs. 3–6.

Discussion: Both simulation results of Fig. 3 show a satisfactory behavior of the AUV, clearly driven to reach and stay on the path. Fig. 4 indicates the evolution of the relative distance between the virtual target and the robot, expressed in the Serret–Frenet frame. The concurrent convergence of $x_{B/F}$ and $y_{B/F}$ to zero confirms the desired behavior of the system. Note that since $x_{B/F}$ converges to zero, the virtual target converges to the closest point on the path. Figs. 5 and 6 show the system velocities' evolution and the related control activity. Concerning

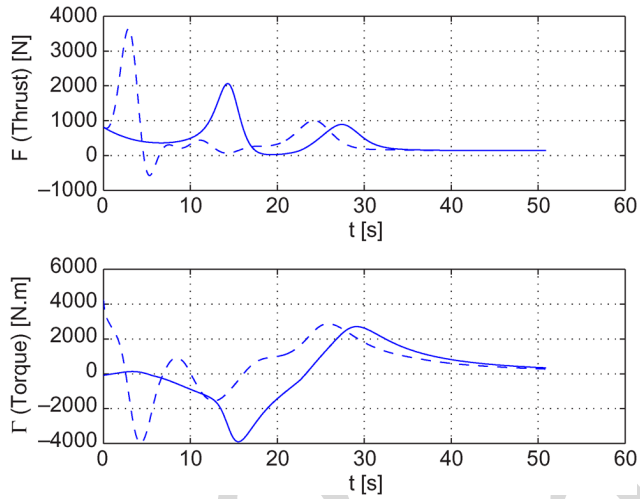

Fig. 6. Control activity, when considering a perfect knowledge of the parameters (simulation 1: solid line; simulation 2: dashed line).

TABLE IV
INITIAL PARAMETERS ESTIMATION

[AU; Please follow the request in Table II]

$m = 3000Kg$	$I_z = 1000N.m.s^2$
$X_{\dot{u}} = -10Kg.$	$Y_{\dot{v}} = -2500Kg.$
$N_{\dot{r}} = -500N.m.s^2$	$X_u = -10Kg.s^{-1}$
$Y_v = -500Kg.s^{-1}$	$N_r = -500N.m.s.$
$X_{u\|u\|} = -10Kg.m^{-1}$	$Y_v\|v\| = -100Kg.s^{-1}$
$N_r\|r\| = -100N.m.s.$	

the amplitude of the control activity, recall that the simulated system is heavy (cf., Table II). Note that the tunable parameters of the proposed control are the control gains K_i, $i = 1, 2, 3, 4$, and the guidance parameters, the asymptotic approach angle, denoted θ_a, and the gain k_δ, designing the smoothness of this approach.

C. Robust Controller

To demonstrate the efficiency of the robust scheme, we first proceed to simulations considering the misestimated parameters of Table IV, without adaptation. The results are given in Figs. 7–10 (dotted lines).

The robust scheme is tested using the path parameters of Table I and the control parameters of Table III. The system parameter estimated values are displayed in Table IV, used to compute the 11 initial values of the parameter groups. The surrounding values for q_1, q_2, and q_4 parameter groups are also considered. The expression of the parameter groups is listed in the Appendix

$$q_1^{\text{up}} = -0.1051, \quad q_1^{\text{down}} = -0.0526$$
$$q_2^{\text{up}} = -0.2534, \quad q_2^{\text{down}} = -0.0676$$
$$q_3^{\text{up}} = 0.5, \quad q_3^{\text{down}} = 0.7.$$

The results are displayed in Figs. 7–10 (straight lines). The adaptation evolution for parameters p_j, $j = 1 \ldots 7$, is given in Figs. 11 and 12, q_i, $i = 1, 2, 3$ in Fig. 13, and d_k, $k = 1 \ldots 4$, in Fig. 14. The convergence gains have been tuned according to

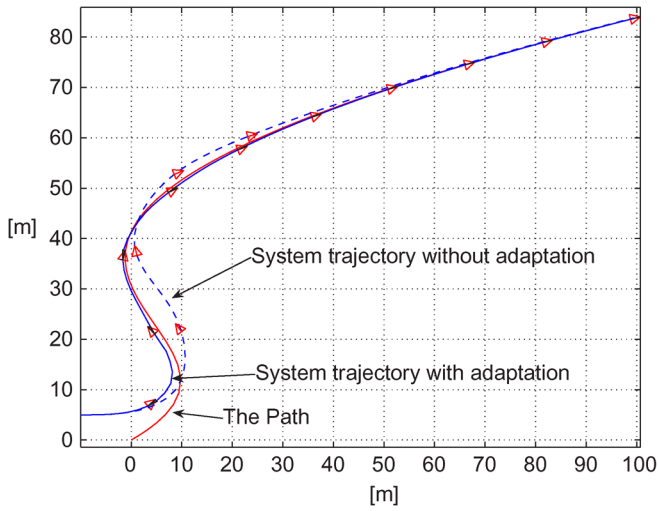

Fig. 7. System trajectories using robust control (solid line) and dynamic control with misestimated parameters (dotted line).

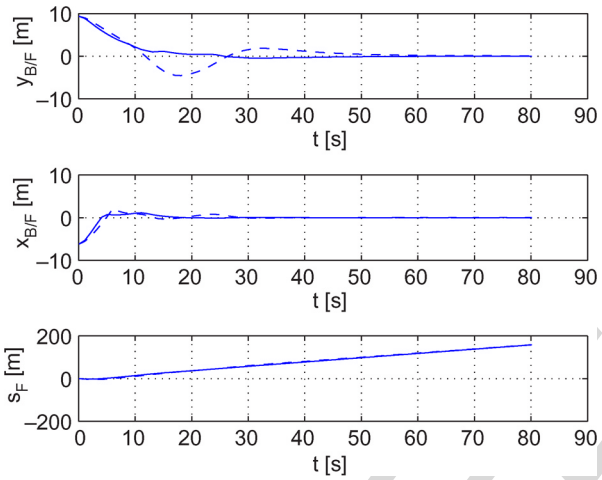

Fig. 8. Relative distance robot/rabit evolution using robust control (solid line) and dynamic control with misestimated parameters (dashed line).

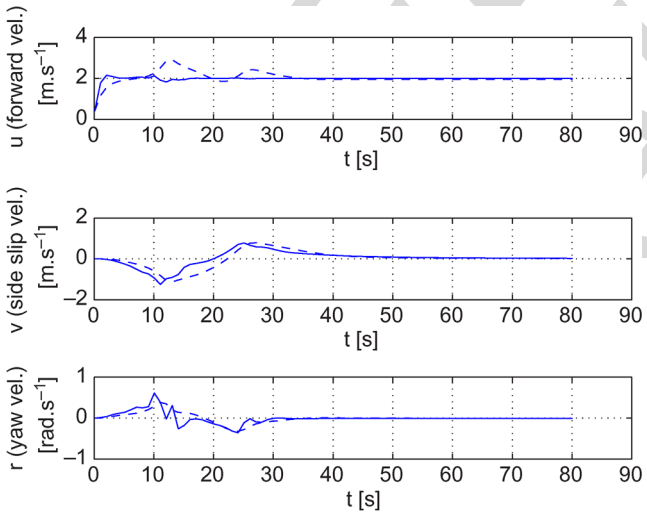

Fig. 9. Velocities evolution using robust control (solid line) and dynamic control with misestimated parameters (dashed line).

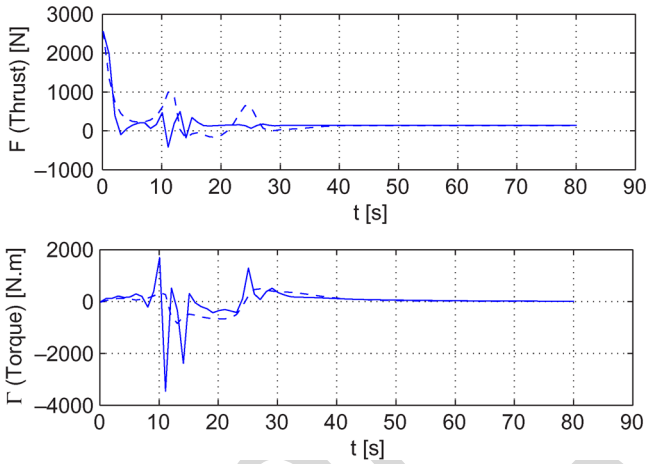

Fig. 10. Control activity, using robust control (solid line) and dynamic control with misestimated parameters (dashed line).

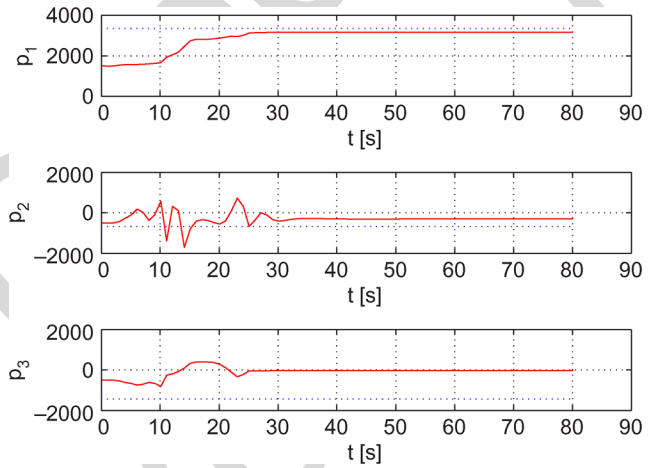

Fig. 11. Evolution of the adaptation of parameters p_i $(i = 1, 2, 3)$ involved in the computation of Γ.

Table V, to observe the convergence of the parameters during the simulation.

Discussion: Trajectories of Fig. 7 clearly indicate the improvement of the robust control with respect to the performances of the dynamic control with misestimated parameters. Note that since the desired path is getting flatter the convergence of the dynamic control is achieved much more later than the robust control results. This compared analysis is confirmed by the evolution of the relative distance between the virtual target and the robot, displayed in Fig. 8, where the convergence evolution of the $y_{B/F}$ variable is similar to the one in the case of a perfect knowledge of the parameters (cf., Fig. 4), which is clearly not the case of the response considering misestimated parameters, without the robust scheme. Fig. 9 indicates also a better convergence of the forward velocity u to the desired one $u_d = 2\ \mathrm{m.s}^{-1}$, when using the robust control. Fig. 10 displays the evolution of the control activity evolution with and without the robust scheme. As expected, the control activity is higher with the robust control. Moreover, the control activity profile of the robust control (solid line) presents some important discontinuities, induced by the switching part of the robust scheme, as one could have expected. The reduction of this chattering effect

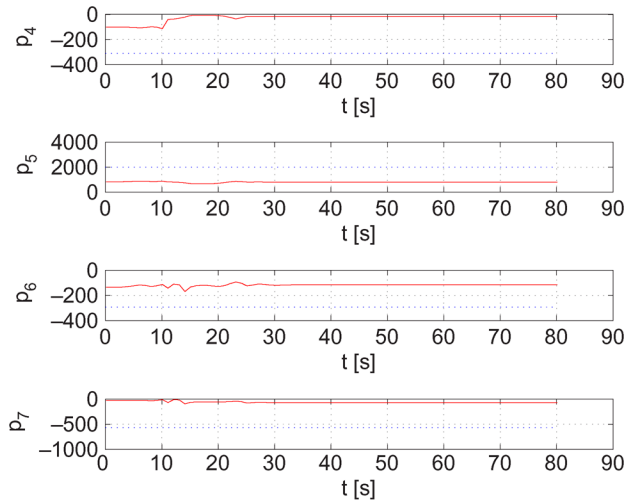

Fig. 12. Evolution of the adaptation of parameters p_i $(i = 4, 5, 6, 7)$ involved in the computation of Γ.

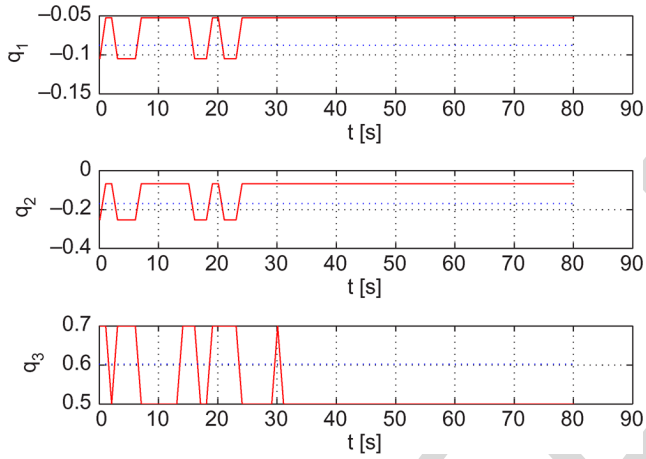

Fig. 13. Evolution of the commutations of parameters involved in the computation of the kinematic reference r_d.

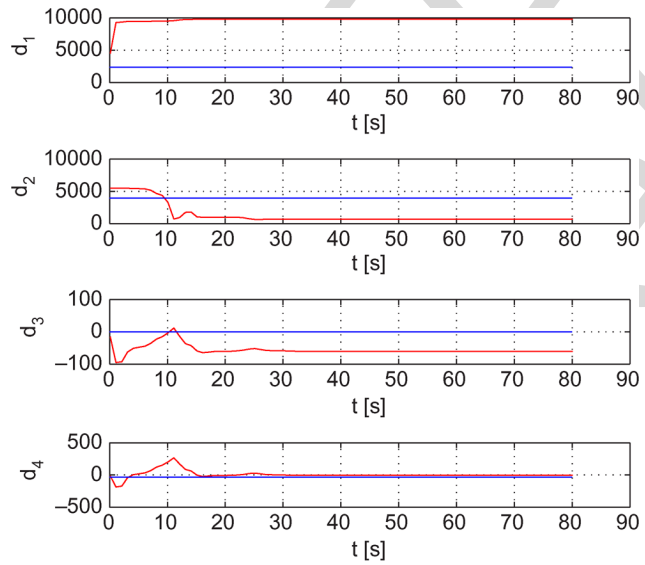

Fig. 14. Evolution of the adaptation of parameters involved in the computation of F.

TABLE V
CONVERGENCE GAINS OF THE ADAPTATION SCHEME

$\lambda_1^p = 30$	$\lambda_2^p = 50$	$\lambda_3^p = 50$	$\lambda_4^p = 10$
$\lambda_5^p = 10$	$\lambda_6^p = 5$	$\lambda_7^p = 8$	$\lambda_1^d = 100$
$\lambda_2^d = 500$	$\lambda_3^d = 1$	$\lambda_4^d = 2$	

TABLE VI
KINEMATIC REFERENCE PARAMETER GROUPS AND FUNCTIONS

q_1 and g_1	q_2 and g_2	q_3 and g_3
$\frac{Y_v}{m_v}$	$\frac{Y_{v\|v\|}}{m_v}$	$\frac{m_{ur}}{m_v}$
$\frac{uv}{v_t^2}$	$\frac{uv\|v\|}{v_t^2}$	$\frac{u^2}{v_t^2}$

TABLE VII
FORWARD CONTROL PARAMETER GROUPS AND FUNCTIONS

d_1 and l_1	d_2 and l_2
m_u	m_{uv}
$\dot{u}_d - K_5(u - u_d)$	$-vr$
d_3 and l_3	d_4 and l_4
X_u	$X_{u\|u\|}$
$-u$	$-u\|u\|$

TABLE VIII
HEADING CONTROL PARAMETER GROUPS AND FUNCTIONS

p_1 and f_1	p_2 and f_2	p_3 and f_3
m_r	$\frac{m_{ur}m_r}{m_v}$	$\frac{Y_v m_r}{m_v}$
$R_0^{\dot{r}_d} - K_3(r - \tilde{r}_d) - K_5(\theta - \delta)$	$-urR_{\dot{v}}^{\dot{r}_d}$	$vR_{\dot{v}}^{\dot{r}_d}$
p_4 and f_4	p_5 and f_5	p_6 and f_6
$\frac{Y_{v\|v\|}m_r}{m_v}$	m_{uv}	N_r
$v\|v\|R_{\dot{v}}^{\dot{r}_d}$	$-uv$	$-r$
p_7 and f_7		
$N_{r\|r\|}$		
$-r\|r\|$		

could be a substantial improvement of the method. Figs. 11 and 11***[AU: Should it be "Figs. 11 and 12"?]*** show the evolution of parameters p_i, $i = 1, \ldots, 7$, involved in the computation of Γ. It could be noted that the parameters are not converging to their real value. This is expected since the related Lyapunov functions (cf., Section III-D2) that warrants the convergence guaranties of the tracking variables, do not consider the convergence of the parameters to their actual value. This is a known behavior of adaptive control, that is, for the linear case, a problem of excitation of the system. This robust control is not designed to make the parameters estimation, but to desensitize the system properties to the parameters misestimation. Fig. 13 shows the evolution of the parameters involved in the computation of the kinematic reference r_d, according to the designed switching scheme. Note that one of the assumption of the problem is that the system is able to switch infinitively fast, and further research on this topic will include the dwell time property of the system, to establish the practical convergence performance of the method. Indeed, including a realistic dwell time in the study will make it impossible to meet asymptotic convergence property, and only practical convergence will be reachable.

TABLE IX
ELEMENTS OF COMPUTATION OF PARAMETER GROUPS AND FUNCTIONS

$R_0^{\dot{r}_d} = f_0^{r_d}(g_1^0 + g_2^0 + g_3^0)$
$R_{\dot{v}}^{\dot{r}_d} = g_0^{\dot{v}} f_1^{r_d} + f_0^{r_d}(g_1^{\dot{v}} + g_2^{\dot{v}} + g_3^{\dot{v}} + g_4^{\dot{v}} + g_5^{\dot{v}})$
$R_{\dot{u}}^{\dot{r}_d} = g_0^{\dot{u}} f_1^{r_d} + f_0^{r_d}(g_1^{\dot{u}} + g_2^{\dot{u}} + g_3^{\dot{u}} + g_4^{\dot{u}} + g_5^{\dot{u}})$
$R_{\ddot{u}}^{\dot{r}_d} = f_0^{r_d} g_1^{\ddot{u}}$
$R_{\dot{u}.\dot{u}}^{\dot{r}_d} = f_0^{r_d} g_1^{\dot{u}.\dot{u}} + g_0^{\dot{u}} g_1^{\ddot{u}}$
$R_{\dot{u}.\dot{v}}^{\dot{r}_d} = f_0^{r_d} g_1^{\dot{u}.\dot{v}} + g_0^{\dot{v}} g_1^{\ddot{u}}$

TABLE X
ELEMENTS OF COMPUTATION OF PARAMETER GROUPS AND FUNCTIONS

$f_0^{r_d}$	$=$	$\frac{1}{1-q_3\frac{u^2}{v_t^2}}$
$f_1^{r_d}$	$=$	$f_r + \sum_{i=1}^{2} q_i g_i$
g_1^0	$=$	$\frac{\partial^2\dot{\delta}}{\partial y^2}\dot{y}^2 + \frac{\partial\dot{\delta}}{\partial y}(-\frac{\partial c_c}{\partial s}\dot{s}^2$ $-c_c\dot{x}\dot{s} + v_t\cos\theta(r - c_c\dot{s})$ $-c_c x K_2\dot{x} + c_c x\sin\theta v_t(r - c_c\dot{s}))$
g_2^0	$=$	$K_1(\dot{\delta} - (r - c_c\dot{s}))$
g_3^0	$=$	$\frac{\partial c_c}{\partial s}\dot{s}^2 + c_c(K_2\dot{x} - \sin\theta v_t(r - c_c\dot{s}))$
$g_0^{\dot{v}}$	$=$	$\frac{q_3}{(1-q_3 g_3)^2}(-\frac{2u^2 v}{v_t^4})$
$g_0^{\dot{u}}$	$=$	$\frac{q_3}{(1-q_3 g_3)^2}(\frac{2uv^2}{v_t^4})$
$g_1^{\dot{v}}$	$=$	$\frac{\partial\dot{\delta}}{\partial y}\frac{1}{v_t}(\sin\theta v + \cos\theta u$ $-c_c x(\cos\theta v - \sin\theta u))$
$g_1^{\dot{u}}$	$=$	$\frac{\partial\dot{\delta}}{\partial y}\frac{1}{v_t}(\sin\theta u - \cos\theta v$ $-c_c x(\cos\theta u + \sin\theta v))$
$g_2^{\dot{v}}$	$=$	$-K_1\frac{u}{v_t^2}$
$g_2^{\dot{u}}$	$=$	$-K_1\frac{v}{v_t^2}$
$g_3^{\dot{v}}$	$=$	$\frac{c_c}{v_t}(\cos\theta v - \sin\theta u)$
$g_3^{\dot{u}}$	$=$	$\frac{c_c}{v_t}(\cos\theta u + \sin\theta v)$
$g_4^{\dot{v}}$	$=$	$q_1\frac{u(u^2-v^2)}{v_t^4}$
$g_4^{\dot{u}}$	$=$	$q_1\frac{v(v^2-u^2)}{v_t^4}$
$g_5^{\dot{v}}$	$=$	$q_2\frac{2u^3\lvert v\rvert}{v_t^4}$
$g_5^{\dot{u}}$	$=$	$q_2\frac{v\lvert v\rvert(v^2-u^2)}{v_t^4}$
$g_1^{\ddot{u}}$	$=$	$\frac{v}{v_t^2}$
$g_1^{\dot{u}\dot{v}}$	$=$	$\frac{u^2-v^2}{v_t^4}$
$g_1^{\dot{u}\dot{u}}$	$=$	$\frac{-2uv}{v_t^4}$

V. CONCLUSION

We have developed a dynamic robust path-following AUV control that exhibits good performances. The proposed method uses a hybrid robust scheme, relying on classic adaptation scheme design of those dynamic parameters that appear with an affine form, and on switching control for the others. A robot design limitation reduces the application field of this solution to torpedo-shaped vehicles that ensure that the ratio m_u/m_v stays far from 1. The asymptotic convergence of the controlled system is shown in the Lyapunov sense. To complete this study, disturbance rejection and unmodeled dynamic robustness must be explicitly addressed, with the introduction of a dwell time, the shortest switching period of the system. Another approach is now under study, relying exclusively on switching system theory. This warrants further research.

APPENDIX
FUNCTIONS AND PARAMETER GROUPS

In the sequel, we present the expression of the functions and parameter group used in Section III-D.

A. Kinematic Reference

The kinematic references, denoted r_d, is rewritten according to (19), where functions g_i and parameter groups q_i, $i = 1, 2, 3$, have the following expression, displayed in Table VI.

B. Forward Control F

The expression of the forward control, denoted F, is rewritten according to (24), where functions l_i and parameter groups d_i, $i = 1, 2, 3, 4$, are expressed in Table VII.

C. Heading Control Γ

The expression of the torque control, denoted Γ, is rewritten according to (29), where functions f_i and parameter groups p_i, $i = 1, \ldots, 7$, are expressed in Tables VIII–X.

ACKNOWLEDGMENT

The authors would like to thank Prof. A. Pascoal and his team for their helpful comments.

REFERENCES

[1] ***[AU: Please provide the referenced pages]***E. Lewis, *Principles of Naval Architecure—Vol III: Motions in Waves and Controllability*. New York: Society of Naval Architects and Marine Engineers (SNAME), 1989.

[2] L. Ji-Hong and L. Pan-Mook, "Design of an adaptive nonlinear controller for depth control of an autonomous underwater vehicle," *Ocean Eng.*, vol. 32, no. 17–18, pp. 2165–2181, 2005.

[3] T. Prestero, "Verification of a six degree of freedom simulation model for the REMUS autonomous underwater vehicle" M.S. thesis, Ocean Mech. Eng., Massachusetts Inst. Technol./Woods Hole Ocean. Inst., Cambridge, MA, Sep. 2001 [Online]. Available: http://www.mit.edu/tprester/main.pdf

[4] D. Soetanto, L. Lapierre, and A. Pascoal, "Adaptive, non-singular path following control of a wheeled robot," in *Proc. IEEE Conf. Decision Control*, Maui, HI, Dec. 9–12, 2003, pp. 1765–1770.

[5] A. Healey and D. Lienard, "Multivariable sliding mode control for autonomous diving and steering of unmanned underwater vehicles," *IEEE J. Ocean. Eng.*, vol. 18, no. 3, pp. 327–339, Jul. 1993.

[6] L. Lapierre, D. Soetanto, and A. Pascoal, "Non-linear path-following control of an AUV," in *Proc. IEEE Conf. Decision Control*, Maui, HI, Dec. 9–12, 2003, pp. 1256–1261.

[7] M. Krstic, I. Kanellakopoulos, and P. Kokotovic, *Nonlinear and Adaptive Control Design*. New York: Wiley, 1995.

[8] F. Song and S. Smith, "Design of sliding mode fuzzy controllers for an autonomous underwater vehicle without system model," in *Proc. MTS/IEEE OCEANS Conf.*, Providence, RI, Sep. 9–14, 2000, pp. 835–840.

[9] W. Naeem, R. Sutton, and S. Ahmad, "Pure pursuit guidance and model predictive control of an autonomous underwater vehicle for cable/pipeline tracking," *IMarEST J. Mar. Sci. Environ.*, no. 1, pt. C, pp. 15–25, Mar. 2004.

[10] ***[AU: Please define UKACC]***W. Naeem, "Model predictive control of an autonomous underwater vehicle," in *Proc. UKACC Postgraduate Symp.*, Sheffield, U.K., Sep. 2002, pp. 19–23.

[11] T. Salgado-Jmenez, J. Spiewak, P. Fraisse, and B. Jouvencel, "A robust control algorithm for AUV: Based on a high order sliding mode," in *Proc. MTS/IEEE Int. OCEANS. Conf.*, Kobe, Japan, Nov. 9–12, 2004, pp. 276–281.

[12] ***[AU: Please provide the referenced pages]***J. Slotine and W. Li, *Applied Nonlinear Control*. Englewood Cliffs, NJ: Prentice-Hall, 1991.

[13] C. Silvestre, A. Pascoal, and I. Kaminer, "On the design of gain-scheduled trajectory tracking controllers," *Int. J. Robust Nonlinear Control*, vol. 12, no. 9, pp. 797–839, Jul. 2002.

[14] ***[AU: Please provide department]***M. Kim, "Nonlinear control and robust observer design for marine vehicles," Ph.D. dissertation, Virginia Polytech. Inst. State Univ., Blacksburg, VA, Nov. 3, 2000.

[15] ***[AU: Please provide the referenced pages]***T. Fossen, *Guidance and Control of Ocean Vehicles*. New York: Wiley, 1994.

[16] M. Aucher, "Dynamique des sous-marins," Paris, France, Internal Rep., science et technique de l'armement, 55, 4 fasc, 1981.

[17] L. Lapierre, D. Soetanto, and A. Pascoal, "Nonsingular path following control of a unicycle in the presence of parametric modelling uncertainties," *Int. J. Robust Nonlinear Control*, vol. 16, no. 10, pp. 485–503, Apr. 2006.

[18] P. Encarnacao, A. Pascoal, and M. Arcak, "Path following for autonomous marine craft," in *Proc. 5th IFAC Conf. Mar. Craft Maneuver. Control*, Aalborg, Denmark, Aug. 2000, pp. 117–122.

[19] P. Encarnacao, A. Pascoal, and M. Arcak, "Path following for marine vehicle in the presence of unknown currents," in *Proc. 6th IFAC Symp. Robot Control*, Vienna, Austria, Dec. 2000, vol. II, pp. 469–474.

[20] A. Aguiar, A. Atassi, and A. Pascoal, "Regulation of a non-holonomic dynamic wheeled mobile robot with parametric modeling uncertainty using Lyapunov function," in *Proc. 39th IEEE Conf. Decision Control*, Sydney, Australia, Dec. 2000, vol. 3, pp. 2995–3000.

[21] ***[AU: Please define IST/ISR]***A. Aguiar, "Nonlinear motion control of non-holonomic and underactuated systems," Ph.D. dissertation, IST/ISR, Lisbon, Portugal, Apr. 2002.

[22] N. Andreff, B. Espiau, and R. Horaud, "Visual servoing from line," Tech. Rep. INRIA n4226, Jul. 2001 [Online]. Available: http://www.inria.fr/rrrt/rr-4226.html

[23] C. Canudas de Wit, H. Khennouf, and C. Samson, "Non-linear control design for mobile robots," in *Recent Trends in Mobile Robotics*, ser. Robotics and Automated Systems, Y. F. Zheng, Ed. Singapore: World Scientific, vol. 11, pp. 121–156.

[24] ***[AU: Please provide page range]***F. Diaz del Rio, G. Jimenez, J. Sevillano, S. Amaya, and A. Balcells, "A new method for tracking memorized paths: Application to unicycle robots," in *Proc. 10th Mediterranean Conf. Control*, Lisbon, Portugal, Jul. 9–12, 2002.

[25] ***[AU: Please provide referenced pages]***W. E. Dixon, D. M. Dawson, E. Zergeroglu, and A. Behal, "Non linear control of wheeled robots," in *Lecture Notes in Control and Information Sciences*. Berlin, Germany: Springler-Verlag, 2001, vol. 262.

[26] ***[AU: Please define IST/ISR]***P. M. Encarnao, "Non linear path following control systems for ocean vehicles," Ph.D. dissertation, IST/ISR, Lisbon, Portugal, Apr. 2002.

[27] J. Hespanha, D. Liberzon, and A. Morse, "Logic-based switching control of an non-holonomic system with parametric modeling uncertainty," *Syst. Control Lett.*, vol. 38, Special Issue on Hybrid Systems, no. 3, pp. 167–177, 1999.

[28] S. Hutchinson, G. D. Hager, and P. I. Corke, "A tutorial on visual servo control," *IEEE Trans. Robot. Autom.*, vol. 12, no. 5, pp. 651–670, Oct. 1996.

[29] ***[AU: Please provide referenced pages]***H. K. Khalil, *Nonlinear Systems*, 3rd ed. Upper Saddle River, NJ: Prentice-Hall, 1996.

[30] ***[AU: Please provide referenced pages]***M. Krstic, I. Kanellakopoulos, and P. Kokotovic, *Non-Linear and Adaptive Control Design*. New York: Wiley, 1995.

[31] ***[AU: Please provide page range]***L. Lapierre, D. Soetanto, and A. Pascoal, "Adaptive, non-linear vision-based path following control of a wheeled robot," in *Proc. 10th Mediterranean Conf. Control*, Lisbon, Portugal, Jul. 9–12, 2002.

[32] D. Liberzon, "Control using logic and switching, part 1: Switching in systems and control," in *Handout Notes of the CDC 01 Workshop*, September 4–7, 2001 [Online]. Available: http//:black.csl.uiuc.edu/liberzon

[33] A. Micaelli and C. Samson, "Trajectory tracking for a unicycle-type and two steering wheels mobile robots," Tech. Rep. INRIA n2097, Nov. 1993 [Online]. Available: http://www.inria.fr/rrrt/rr-2097.html

[34] C. Samson and A. Abderrahim, "Mobile robot control part 1: Feedback control of a non-holonomic mobile robot," Tech. Rep. INRIA n1281, Jun. 1991 [Online]. Available: http://www.inria.fr/rrrt/rr-1288.html

[35] ***[AU: Please provide referenced pages]***R. Sepulchre, M. Jankovic, and P. Kokotovic, *Constructive Non-Linear Control*. New York: Springler-Verlag, 1997.

[36] ***[AU: Please provide university and department]***C. Silvestre, "Multi-objective optimization theory with application to the integrated design of controllers/plants for autonomous vehicle," Ph.D. dissertation, Lisbon, Portugal, Jun. 2000.

[37] J. J. Slotine and W. Li, *Applied Non-Linear Control*. Englewood Cliffs, NJ: Prentice-Hall, 1995, pp. 125–128.

[38] ***[AU: Please provide page range]***D. Soetanto, L. Lapierre, and A. Pascoal, "Path-following control for a non-holonomic mobile robot with parametric modeling uncertainties," in *Proc. Eur. Control Conf.*, Cambridge, U.K., Sep. 1–4, 2003.

[39] ***[AU: Please provide page range]***D. Soetanto, L. Lapierre, and A. Pascoal, "Non-singular path-following control of a unicycle-type vehicle in presence of parametric modeling uncertainties," in *Proc. Int. Conf. Adv. Robot.*, Coimbra, Portugal, Jun. 30–Jul. 3 2003.

Lionel Lapierre received the Ph.D. degree ***[AU: In what field of study?]***from the University of Montpellier 2, Montpellier, France, in 1999.

Then, he joined the team of Prof. A. Pascoal within the European project FreeSub for three years. Since 2003, he has been with the Underwater Robotics Division, Laboratoire d'Informatique, de Robotique et de Microélectronique de Montpellier (LIRMM), Montpellier, France.

Bruno Jouvencel was born on February 3, 1955, in Paris, France. He graduated from the Electronical Engineering Department, Ecole Normale Supérieure, Cachan, France, in 1981 (Agrégation de Génie Electrique). He received the Ph.D. degree in perception systems for robotic manipulators in automatic control from Montpellier University, Montpellier, France***[AU: In what year?]***.

Currently, he is a Full Professor at Montpellier University and Researcher at the Laboratoire d'Informatique, de Robotique et de Microélectronique de Montpellier (LIRMM), Montpellier, France. In 2004, he was elected member of the National Committee, which evaluates French research laboratories in communication and information technologies (Section 07 of the Comité National de la Recherche Scientifique). For ten years, he has worked on the design, the command, and the perception of autonomous underwater vehicles. A first prototype TAIPAN 1 has been developed in 1998 and a second vehicle "H160" was conceived and realized in partnership with an industrial company.

Robust Nonlinear Path-Following Control of an AUV

Lionel Lapierre and Bruno Jouvencel

***Abstract*—This paper develops a robust nonlinear controller that asymptotically drives the dynamic model of an autonomous underwater vehicle (AUV) onto a predefined path at a constant forward velocity. A kinematic controller is first derived, and extended to cope with vehicle dynamics by resorting to backstepping and Lyapunov-based techniques. Robustness to vehicle parameter uncertainty is addressed by incorporating a hybrid parameter adaptation scheme. The resulting nonlinear adaptive control system is formally shown and it yields asymptotic convergence of the vehicle to the path. Simulations illustrate the performance of the derived controller.**

***Index Terms*—Adaptive control, nonlinear control, path following, underactuated vehicle.**

I. Introduction

THE design of a nonlinear path-following controller autonomous underwater vehicle (AUV) involves two different problems: the path-following strategy and the control of an underactuated vehicle.

A. Path Following

Path following requires the vehicle to reach and follow a desired path without time constraint. This is done by controlling the forward velocity to converge to a desired value (constant in our case), and acting on the vehicle's orientation to drive it onto the path. The problem is considered to be solved when the designed controller guarantees asymptotic convergence to the path. Many papers have addressed the problem of path-following control for a nonholonomic wheeled vehicle, in most cases a unicycle-type robot [25], [33], [34]. The underlying questions to be solved concern the following.

1) *Path parameterization.* If the path can be considered as straight lines or circles, classic geometrical description may be used to parameterize the path and in the control design [22], [28], [31]. The most general parameterization considers the curvature of the path in function of the curvilinear abscissa of the target point [20], [33], [34].
2) *Choice of the target point on the path.* The choice of the target point implies different control strategies. In [33], the target point is designed to be the closest point on the path, relative to the current position of the robot. This allows a rapid convergence to the path, since the distance to the path is minimal. However, this method implies a drastic limitation to the robot's initial conditions. Since the target point is defined with respect to the current position of the robot, it has to be actualized at each instant of time, and problems occur when the robot is located at the center of the path curvature (the target point is no longer unique) or during a movement that potentially passes close to it (the computation of the current reference is not well posed). To solve this problem, a very conservative but necessary condition is used: the initial position of the robot must be such that the initial distance to the path is *smaller than the smallest radius of curvature present on the path*. Another solution [24], [39] consists in considering the target point as a virtual moving target, animated on the path with its own movement laws. To ensure cooperative behavior of the target (slowing down when the vehicle is behind and accelerating when the vehicle is in advance), the movement equations of the target are related to the velocity of the robot. This implies that the target exponentially converges to the closest point on the path, with the difference that the target point is now well defined, even if the vehicle crosses the current center of curvature. The previous constraint is relaxed into the following: the initial position of the vehicle should be*far from the center of curvature relative to the initial position of the target point on the path*.

B. Control of an Underactuated Vehicle

An increasing number of papers have addressed the topic of the control of ocean vehicles. Vehicles designed to accomplish long-range missions (AUVs, ships) are generally underactuacted, or in the case of fully actuated vehicles, the inefficiency of a side thruster during high-velocity forward movement leads them to be considered as underactuated. This implies that transverse movement (sway) is not directly controlled.

In the case of a wheeled robot, the transverse ground friction of the wheels, expressing the nonholonomic constraint, effectively cancels this behavior. Nevertheless, in underwater or terrestrial plane applications, the control inputs are the same: the forward and yaw velocities. This explains the connection between unicycle-type robots and AUV path-following control strategies. For a unicycle-type robot path-following control, please refer to [31], [33], [34], and [23].

The similarity between these two vehicles ends on considering that the resulting total velocity of the underwater robot is not aligned with its main direction of movement. This implies that the AUV heading is not permanently tangent to its trajectory, but the strategy of controlling the amplitude and the orientation of the total velocity holds, underlying the added necessity of having a measurement, or a satisfactory estimation,

Manuscript received January 5, 2006; revised May 31, 2007; accepted February 26, 2008. This work was supported by the EC under Project FREESUB***[AU: Please define EC and FREESUB]***.

Associate Editor: D. Stilwell.

The authors are with the Laboratoire d'Informatique de Robotique et de Microélectronique de Montpellier (LIRMM) Institute, Montpellier 34392, France (e-mail: lapierre@lirmm.fr).

Color versions of one or more of the figures in this paper are available online at http://ieeexplore.ieee.org.

Digital Object Identifier 10.1109/JOE.2008.923554

of the sway velocity [21], [26]. Path-following systems for marine vehicles have been reported by Encarnacao *et al.* in [18], and [19], where the underlying assumption was that the vehicle's forward speed tracks a desired speed profile, while the controller acts on the vehicle's orientation to drive it to the path***[AU: "speed" and "velocity" are used interchangeably in the paper. Can "speed" be used throughout?]***. Typically, smoother convergence to a path is achieved, in comparison with performances obtained with a trajectory-tracking controller, and the control signals are less often pushed to saturation [17].

Because the AUV controller relies on a dynamic model of the system, the performances achieved are dependent on the accuracy of the estimation of model parameters. Nevertheless, precise modeling for an AUV is a difficult task, and it results in a set of highly coupled nonlinear equations. For more information on a subject of modeling, the reader should refer to [16] and [15].

Designing a controller to regulate such a nonlinear model is not a simple process, and classic linear approaches do not lead to satisfactory performances [14]. Meanwhile, Silvestre *et al.* [13] propose a gain-scheduled trajectory-tracking controller, based on the fact that the linearization of the system dynamics about trimming trajectory (helices parameterized by the vehicle's linear speed, yaw rate, and flight path angle) results in a time-invariant plant. Then, considering a global trajectory consisting of the piecewise union of trimming trajectories, the problem is solved by designing a family of linear controllers for the linearized plants at each operating point. Interpolating between these controllers guarantees adequate local performance for all linearized plants. Nevertheless, this methodology does not explicitly address the issues of global stability and performance.

Because model estimation accuracy cannot be absolutely guaranteed, the robustness of the control scheme is of major importance. One of the classic control methods relies on the sliding-mode design [12]. In [11], Salgado *et al.* propose a control design applied to the Taipan 2 AUV, based on an high-order sliding mode, that explicitly addresses the classic chattering problem encountered when using the classic sliding mode. This is achieved by controlling high-order derivatives of the sliding surface, thus removing the discontinuity of the control vector. This method exhibits robust behavior, but the equivalent control is designed using a linearized method that does not allow for global stability and performance analysis. In [8], Song *et al.* combine the sliding-mode advantages with a fuzzy approach expressing the switching rules based on the experimental data. The authors say this method is independent of any system model. Nevertheless, global stability and performance are not addressed. Naem *et al.* [10] and [9] propose a control based on model prediction using genetic algorithms, but the performances and stability properties are not addressed.

Considering model nonlinearities, the Lyapunov approach has many advantages. The first step allows for designing a control solution that takes into account the system kinematics and meets uniform asymptotic convergence requirements. As we will see in the sequel, the concurrent use of the virtual target principle allows for expressing the problem in a nonsingular way, thus guaranteeing the respect of the convergence property whatever the initial conditions are, and meeting a global and uniform asymptotic convergence requirement. The second step consists in using the backstepping approach [7], augmenting the system with its dynamic states, and still meeting global performance requirements. For an application of this method to an underactuacted marine system, please refer to [17]. Another backstepping stage allows parameter uncertainty to be taken into account, in designing an adaptive scheme that guarantees robustness. It should be noted that this method is valid if the parameters appear in an affine form in the control expression. An application to a nonholonomic wheeled system can be found in [4]. The particularity of an AUV system is its underactuation, which leads to a Lyapunov-based control expression, with parameters that do not appear in an affine form [6]. Existing solutions are based on a model simplification, reducing the problem to a multivariable linear system [5], [15], [3], or using a McLaurin series expansion of the trigonometric terms around a well-chosen guidance function [2]. Obviously, these existing methods do not allow for establishing the global convergence property of the solution.

C. Paper Description

The problem formulation is described in Section II. Section III describes the design of an asymptotically convergent kinematic control (Section III-A), extended to cope with vehicle dynamics (Section III-B) by resorting to backstepping and Lyapunov-based techniques (for details on this topic, please refer to [30]). The computation of such a control is shown in Section III-C and it provides a limitation of robot design. Robustness to uncertainty in the parameters of vehicle dynamics is addressed by incorporating a hybrid parameter-adaptation scheme (Section III-D). Section IV provides simulation results of the previously described controllers. Section V contains the conclusions and explanation of future work concerning this subject. It should be noted that this paper does not explicitly address the disturbance rejection problem (e.g., ocean current, waves effect, etc.).

II. Problem Formulation

This section introduces some basic notation, presents the kinematic equations of motion for an underactuated mobile robot, and formalizes the problem of driving the robot along a desired path, in the horizontal plane. The first part (Section II-A) shows the notations adopted throughout this paper. Section II-B describes the underactuated underwater robot, as depicted in Table II. Section II-C presents the kinematic equations of the system. Section II-D briefly presents the dynamic model of the robot. Finally, Section II-E states the problem of finding a controller that guarantees convergence to a desired path, taking into account the parametric uncertainties.

A. Notation

Throughout this paper, the following notations will be used.

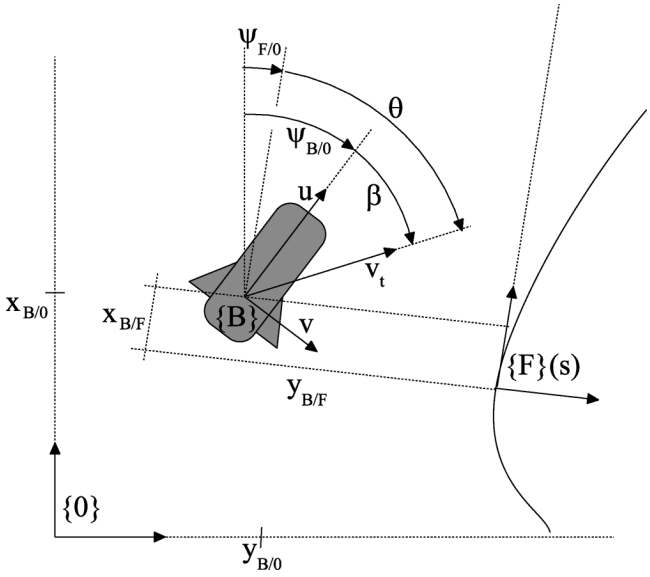

Fig. 1. Frame definition and description of the problem posed.

$\{A\}$ $:= \{x_A\ y_A\ z_A\}$. Reference frame with the origin in A. We let $\{0\}, \{F\}$, and $\{B\}$ be inertial, Serret–Frenet, and body axis frames, respectively.

$p_{A/B}$ $= [x_{A/B}\ y_{A/B}\ z_{A/B}]^T$. Position of the frame $\{A\}$ in relation to $\{B\}$. Note that $\dot{p}^C_{A/B} = [\dot{x}^C_{A/B}\ \dot{y}^C_{A/B}\ \dot{z}^C_{A/B}]^T$ represents the velocity of the frame $\{A\}$ in relation to $\{B\}$ expressed in $\{C\}$.

$\Psi_{A/B}$ Orientation of $\{A\}$ in relation to $\{B\}$, and $\dot{\Psi}_{A/B}$ the angular velocity of $\{A\}$ in relation to $\{B\}$.

R^B_A Rotational matrix from $\{A\}$ to $\{B\}$.

Note that because the study takes place in the horizontal plane, $z_{A/B} =$ constant and $\dot{z}^C_{A/B} = 0, \forall (A, B, C)$.

B. Vehicle Description

The vehicle has two identical rear thrusters, mounted symmetrically with respect to its longitudinal axis of symmetry. Each thruster generates a control force F_i, $i = 1, 2$, and a torque that we consider negligible. The common action mode of the thrusters results in a forward force F, and their differential action mode generates a torque Γ. $[\Gamma F]^T$ defines the dynamic system input.

We assume that the vehicle is neutrally buoyant and that its metacenter coincides with the origin of $\{B\}$. $p_{B/0}$ specifies the absolute position of the origin of $\{B\}$ in $\{0\}$, and $\Psi_{B/0}$ is the parameter that represents the orientation of $\{B\}$ with respect to $\{0\}$, the yaw angle. $\dot{p}^B_{B/0} = [u\ v\ 0]^T$ denotes the absolute velocity of $\{B\}$ with respect to $\{0\}$, expressed in the body frame. u and v are the longitudinal (surge) and transverse (sway or sideslip) velocities, respectively. $\dot{\Psi}_{B/0} = r$ represents the heading velocity (Fig. 1). We also define the sideslip angle as

$$\beta = \arctan(v/u). \tag{1}$$

Note that the well poseness of this expression requires the following assumption:

$$|u| + |v| \neq 0 \Leftrightarrow v_t^2 = u^2 + v^2 \neq 0 \qquad \forall t$$

where v_t is the AUV's total velocity. Note that the control of an AUV system implies considering a permanent positive velocity, therefore the previous condition is covered by the following:

$$v_t > 0 \qquad \forall t. \tag{2}$$

C. Kinematic Model of the Robot

The kinematic model relates the inertial velocity expressed in the body frame $\{B\}$ with the one expressed in the inertial frame $\{0\}$, through the equation $\dot{p}^0_{B/0} = R^0_B . \dot{p}^B_{B/0}$. Extracting the meaningful relations yields

$$\begin{aligned} \dot{x}^0_{B/0} &= u\cos(\Psi_{B/0}) - v\sin(\Psi_{B/0}) \\ \dot{y}^0_{B/0} &= u\sin(\Psi_{B/0}) + v\cos(\Psi_{B/0}) \\ \dot{\Psi}_{B/0} &= r. \end{aligned} \tag{3}$$

Note that $[u\ r]^T$ defines the kinematic system inputs.

D. Dynamic Model of the Robot

The dynamic model of the chosen robot is the classical one described in (4). A complete model of the Infante AUV, developed at the DSOR***[AU: Please define DSOR]***, is described in [36]

$$\begin{aligned} F &= m_u \dot{u} + d_u \\ 0 &= m_v \dot{v} + m_{ur} ur + d_v \\ \Gamma &= m_r \dot{r} + d_r \end{aligned} \tag{4}$$

with

$$\begin{aligned} m_u &= m - X_{\dot{u}}, \quad d_u = -X_{uu}u^2 r - X_{vv}v^2 \\ m_v &= m - Y_{\dot{v}}, \quad d_v = -Y_v uv - Y_{v|v|}v|v| \\ m_r &= I_z - N_{\dot{r}}, \quad d_r = -N_v uv - N_{v|v|}v|v| - N_r ur \\ m_{ur} &= m - Y_r \end{aligned}$$

where m denotes the system mass, I_z is the moment of inertia with respect to the z-axis, and $X_{..}$, $Y_{..}$, and $N_{..}$ are the hydrodynamic derivatives of the system. For more information on the modeling of the Infante vehicle, please refer to [36]. Note that $[F\Gamma]^T$ defines the dynamic system inputs.

E. Problem Formulation

1) Side-Slipping Vehicle Control: The laws of mechanics show that the trajectory of a moving object is fully related to the amplitude and the orientation of its total velocity. These variables must be driven to a desired value to control the trajectory. The control strategy depends on the type of actuation mounted. From the actuation point of view, there exists a visible similarity between the underactuated underwater robot described in Section II-D and the classic nonholonomic wheeled unicycle-type robot. The main difference is that the nonholonomic constraint, active in the wheeled robot, is relaxed in the underactuated system. The direct consequence is that the total

velocity of a unicycle-type robot is permanently equal to its forward velocity u, while the total velocity of an underactuated vehicle results from both surge and sway components u and v [see (2)].

The path-following problem is solved for the unicycle-type robot by designing a control that drives the vehicle onto the path and then insures that the orientation of the forward velocity u stays tangent to the path. In the case of an underactuated vehicle, this is no longer valid. The transverse component of the velocity implies that the robot is not aligned with its total velocity, so while the unicycle case is solved by controlling the forward velocity u, the underactuated case requires the control of the total velocity v_t defined in (2). Designing a controller for a sideslipping vehicle implies driving the amplitude and the orientation of the total velocity to desired values, defined with respect to the path that the robot must reach and follow. The related variables are $\|v_t\|$ and $\theta = \beta + \Psi_{B/F}$. This implies a design limitation on a submarine robot controlled in this way, which is shown in Section III-C. It is because the kinematic controller involves a computation of $\dot{\beta}$, therefore a computation of $\dot{u}$ and $\dot{v}$, the longitudinal and transverse accelerations of the robot. Relying on the dynamic model injects dynamic parameters at the kinematic level. The backstepping process, used to design the dynamic control from the kinematic ***[AU: Kinematic what?]***, reveals the necessary computation of $\ddot{\beta}$, hence $\ddot{u}$ and $\ddot{v}$, the transverse and longitudinal system jerks. Once again, this is achieved using the dynamic model, and it implicitly implies deriving longitudinal and transverse acceleration expression from the dynamical model. This emphasizes the limit of the hypothesis made during the drawing up of the dynamical model, especially the neglected high-order terms. On the other hand, a hybrid adaptation scheme can be designed (Section III-D) that relaxes the necessity for high accuracy in the estimation of the constant model parameters.

2) Path Following: To derive a controller for a path-following problem, the equations of the system must be derived relative to a given path, and the goal of the controller is to drive the robot to reach and follow the path, without time constraint. The parameterization of the problem is illustrated in Fig. 1. Referring to Fig. 1, given any point F on the path, a controller that drives θ to 0, as $x_{B/F}$ and $y_{B/F}$ go to 0, solves the path-following problem. The difference in the strategies that can be adopted concerns the definition of point F. In [33], point F is defined as the closest point on the path with respect to the current position of the robot. In this case, the line (BF) is always perpendicular to the path tangent on F. Thus, the parameterization of the problem is simpler, convergence is guaranteed when $\|BF\|$, and θ are driven to 0. However, this method implies a singularity when point B is located at the center of the path curvature, at point F (θ is undefined). Locate point F by its curvilinear abscissa s_F, and name $c_c(s_F)$ the path curvature at this point. Then, the singularity occurs when $\|BF\| = 1/c_c(s_F)$. In addition, the analysis in [34] shows that global convergence is guaranteed only if $\|BF\| < 1/c_c^{\max}$ for all locations of F, and for $c_c^{\max}$ defining the maximum curvature encountered on the path. This is a very restrictive hypothesis that implies a considerable limitation on the initial condition $\|BF\|_{t=0} < 1/c_c^{\max}$ and a poor disturbance rejection capability. Another solution consists in defining point F as a virtual moving target that describes the path. The movement control of this target introduces a supplementary virtual state into the system, but transforms the previous constraint to $\|BF\|_{t=0} \neq [c_c(s|_{t=0})]^{-1}$. The behavior of the virtual target (captured in the expression of $\dot{s}_F$) is chosen according to the derivation of Lyapunov functions in the backstepping process, and results in a very cooperative target that quickly converges to the closest point on the path. Expressed in the Serret–Frenet frame $\{F\}$, the kinematic equations of the problem are rewritten as

$$\begin{aligned} \dot{x}_{B/F} &= -\dot{s}_F\left(1 - c_c(s_F)y_{B/F}\right) + v_t\cos\theta \\ \dot{y}_{B/F} &= -c_c(s_F)\dot{s}_F x_{B/F} + v_t\sin\theta \\ \dot{\theta} &= r + \dot{\beta} - c_c(s_F)\dot{s}_F. \end{aligned} \tag{5}$$

3) Mathematical Formulation: Equipped with this formalism ***[AU: Formulation?]***, we can now state the kinematic control problem $\mathbf{C_1}$ that is addressed in Section III-A.

> $\mathbf{C_1}$: Given the robot kinematic model (3), the robot dynamic model (4), and a set of available measurements coming from robot sensors, compute $U_{kin} = [u(.)\ r(.)\ \dot{s_F}]^T$, so that $\theta, x_{B/F}$, and $y_{B/F}$ converge to 0 as t goes to ∞.

This problem will be extended in Section III-B to explicitly deal with vehicle dynamics. The dynamic control problem $\mathbf{C_2}$ is stated as follows.

> $\mathbf{C_2}$: Given the robot kinematic model (3), the robot dynamic model (4), and a set of available measurements coming from robot sensors, compute $U_{\text{dyn}} = [F(.)\ \Gamma(.)\ \dot{s_F}]^T$, so that $\theta, x_{B/F}$, and $y_{B/F}$ converge to 0 as t goes to ∞.

Note that the validity of statement $\mathbf{C_2}$ implies that there is no external disturbance, sensor noise, or unmodeled dynamics, and a perfect knowledge of the system parameters. Consider that there is no external disturbances, sensor noise, or unmodeled dynamics, but that the parameters are not perfectly known. Section III-C describes another version of the dynamic controller that guarantees robustness against parameter uncertainty and solves problem $\mathbf{C_3}$, stated as follows.

> $\mathbf{C_3}$: Given the robot kinematic model (3), the robot dynamic model (4), a set of available measurements coming from robot sensors, and a set of reasonable estimation of the nine parameters of the dynamic model, compute $U_{\text{dyn}}^{Rbst} = [F(.)\ \Gamma(.)\ \dot{s_F}\ \dot{p_i}]^T$, so that $\theta, x_{B/F}$, and $y_{B/F}$ converge to 0 as t goes to ∞.

The effects of external disturbance, sensor noise, or unmodeled dynamics are not treated in this paper. The solution consists in proving the boundedness of the system output in the presence of bounded external disturbance and unmodeled dynamics effect, and extracting from the expression of the bounded system output the meaningful information related to the performance of the controlled system.

A proposed solution for problems $\mathbf{C_i}$ $(i = 1, 2, 3)$ is described in the following section.

III. Controller Design

This section describes the solutions to problems $\mathbf{C_1}$, $\mathbf{C_2}$, and $\mathbf{C_3}$, stated in the previous section. In the following, we will extensively use a corollary of Barbalat's lemma (CBL), and LaSalle's theorem, stated as follows.

Barbalat's Lemma: If $f(t)$ is a double differentiable function such that $f(t)$ is finite as t goes to ∞, and such that $\dot{f}(t)$ is uniformly continuous, then $\dot{f}(t)$ tends to 0 as t tends to ∞.

Uniform Continuity Sufficient Condition: $\dot{f}(t)$ is uniformly continuous if $\ddot{f}(t)$ exists and is bounded.

Corollary of Barbalat's Lemma: If $f(t)$ is a double differentiable function such that $f(t)$ is finite as t goes to ∞, and such that $\ddot{f}(t)$ exists and is bounded, then $\dot{f}(t)$ tends to 0 as t tends to ∞.

LaSalle's Theorem: Let Ω be a positively invariant set of the system described in (3) and (4). Suppose that every solution starting in Ω converges to a set $E \subset \Omega$ and let M be the largest invariant set contained in E. Then, every bounded solution starting in Ω converges to M as t tends to ∞.

For details of Barbalat's lemma and its application, please refer to [37]. For demonstration and application of LaSalle's theorem, please refer to [35] and [29]. Note that the application of LaSalle's theorem is restricted to autonomous systems. In our situation, the fact that the desired forward velocity is constant allows us to consider our system as autonomous.

A. Kinematic Controller

With the formalism developed previously, we may now state the following theorem.

Proposition 1: Consider the robot models (3) and (4) and let a desired approach angle be defined by

$$\delta(y_{B/F}) = -\theta_a \frac{e^{2k_\delta y_{B/F}} - 1}{e^{2k_\delta y_{B/F}} + 1} \tag{6}$$

where k_δ is a positive gain and $0 < \theta_a < \pi/2$. Further, assume that measurements of $[u\ v]^T$ are available from robot sensors and that a parameterization of the path is available such that given s_F, the curvilinear abscissa of a point on the path, the variables $\theta, x_{B/F}, y_{B/F}$, and $c_c(s_F)$ are well defined and computable. Then, the control law

$$U_{kin} = \begin{cases} r = \dot{\delta} - \dot{\beta} - K_1(\theta - \delta) + c_c(s_F)\dot{s}_F \\ \dot{s_F} = \cos\theta v_t + K_2 x_{B/F} \end{cases} \tag{7}$$

solves problem $\mathbf{C_1}$, with K_1, K_2, and k_δ three arbitrary positive gains, the assumption that $v_t > 0, \forall t$, and given the initial relative position $[\theta, x_{B/F}, y_{B/F}]|_{t=0}$.

Proof: The proof is structured in three parts. First, we show that the system asymptotically follows the reference angle δ. Then, we show that the reference asymptotically drives the robot onto the path. Finally, we use the LaSalle invariance principle to concatenate the two previous convergence properties.

Consider the following Lyapunov function $V_1 = (1/2)(\theta - \delta)^2$. It is straightforward to show that the choice of the control

$$r = \dot{\delta} - \dot{\beta} - K_1(\theta - \delta) + c_c(s_F)\dot{s}_F$$

yields $\dot{V}_1 = -K_1(\theta - \delta)^2 \leq 0$. That is, V_1 is a positive and monotonically decreasing function up to a well-defined limit

$$\lim_{t\to\infty} V_1 = l_1. \tag{8}$$

Simple derivation shows that $\ddot{V}_1 = 2K_1^2(\theta - \delta)^2$, which is bounded since (8). Then, using the CBL, we conclude that $\lim_{t\to\infty} \dot{V}_1 = 0$. That is

$$\lim_{t\to\infty} \theta = \delta|_{t\to\infty}. \tag{9}$$

The system asymptotically follows the reference $\delta(y_{B/F})$ defined in (6), so the trajectories of the system will asymptotically reach the invariant set E defined as

$$E := \left((x_{B/F}, y_{B/F}) \in \Re^2, \dot{V}_1 = 0\right). \tag{10}$$

For the sake of clarity, define $x = x_{B/F}$, $y = y_{B/F}$, and $s = s_F$, and recall (5). Study the trajectories of the system onto the invariant set E. Consider the Lyapunov candidate $V_E = (1/2)(x^2 + y^2), \forall (x, y) \in E$. It is straightforward to show that the choice

$$\dot{s} = v_t \cos\theta + K_2 x \tag{11}$$

leads to

$$\dot{V}_E = y v_t \sin\delta - K_2 x^2 < 0 \qquad \forall ((x, y) \neq 0) \in E \tag{12}$$

since onto the set ***[AU: Delete "onto"? It is unclear here. Please rewrite.]*** $E : \theta = \delta$, $sign(\delta) = -sign(y)$, $\delta \in [-\theta_a\ \theta_a]$, $0 < \theta_a \leq \pi/2$, and using the assumption $\lim_{t\to\infty} v_t > 0$, covered by the necessary assumption for the definition of (2). Therefore, V_E is finite.

Moreover, it is straightforward to show that $\ddot{V}_E$ is bounded, and we use the CBL to prove that $\lim_{t\to\infty} \dot{V}_E = 0$, which implies $\lim_{t\to\infty} y = 0$ and $\lim_{t\to\infty} x = 0$, since (12). Hence, $(x, y) = (0, 0)$ is the unique stable point of E, and every trajectory of the system starting in E asymptotically converges to the origin.

We now use LaSalle's invariance principle. Let $\Omega = \Re^2$. The first part of the proof showed that every solution starting in Ω asymptotically converges to E. The second step showed that the largest invariant set of E is $M = [(x, y) = 0^2]$, so every bounded solution starting in Ω converges to 0 as t tends to ∞. ■

B. Dynamic Controller

The development of the dynamic control is based on the previous result, considering the kinematic control as a reference, called r_d, for the dynamic control

$$\begin{cases} r_d = \dot{\delta} - K_1(\theta - \delta) - \dot{\beta} + c_c(s)\dot{s} \\ \dot{s} = \cos\theta v_t + K_2 x_{B/F}. \end{cases} \tag{13}$$

Let $\epsilon_r = r - r_d$ and consider the Lyapunov candidate V_2

$$V_2 = K_5 V_1 + \frac{1}{2}\epsilon_r^2 + \frac{1}{2}(u - u_d)^2 \tag{14}$$

with K_5 being a positive gain. Simple computations show that

$$\begin{cases} \dot{r} = \dot{r_d} - K_3(r - r_d) - K_5(\theta - \delta) \\ \dot{u} = \dot{u_d} - K_4(u - u_d) \end{cases} \tag{15}$$

where $\dot{u}_d = 0$ in our study case. Recall that $\dot{\theta} = r - c_c\dot{s} + \dot{\beta}$, then

$$\dot{V}_2 = -K_1K_5(\theta - \delta)^2 - K_3(r - r_d)^2 - K_4(u - u_d)^2 \leq 0.$$

Note that this condition is more restrictive than necessary. The condition that the desired velocity profile is invariant is enough. It is now straightforward to compute the control inputs F and Γ by solving the dynamics (4) to obtain

$$U_{\text{dyn}} = \begin{cases} \Gamma = m_r\Big(\ddot{\delta} - \ddot{\beta} - (K_1 + K_3)(\dot{\theta} - \dot{\delta}) - (K_5 + K_1K_3) \\ \qquad \times(\theta - \delta) + c_c\ddot{s} + \dfrac{\partial c_c}{\partial s}\dot{s}^2\Big) + d_r \\ F = m_u\left(\dot{u_d} - K_4(u - u_d)\right) + d_u. \end{cases} \tag{16}$$

We can now state Proposition 2 that solves problem $\mathbf{C_2}$.

Proposition 2: Consider the robot models (3) and (4) and the desired approach angle defined in (6), where k_δ is a positive gain and $0 < \theta_a < \pi/2$. Further, assume that measurements of $[u\ v\ r]^T$ are available from robot sensors and that a parameterization of the path is available such that, given s, the curvilinear abscissa of a point on the path, the variables $\theta, x_{B/F}, y_{B/F}, c_c, (\partial c_c/\partial s)$ are well defined and computable. Define u_d as the desired forward velocity. Then, control law (16) and expression (7), with K_1, K_2, K_3, K_4, and K_5 positive gains, the assumption that $v_t > 0, \forall t$, and given the initial relative position $[\theta, x_{B/F}, y_{B/F}]|_{t=0}$, solve problem $\mathbf{C_2}$.

Proof: Considering the V_2 (14) Lypaunov function, and using the CBL, as previously, it is straightforward to show that

$$\begin{aligned} &\lim_{t\to\infty}\theta = \delta|_{t\to\infty} \\ &\lim_{t\to\infty}\dot{\theta} = \dot{\delta}|_{t\to\infty} \\ &\lim_{t\to\infty}u = u_d. \end{aligned}$$

Thus, the trajectories of the system will reach the invariant set E

$$E := \left((x_{B/F}, y_{B/F}) \in \Re^2, \dot{V}_2 = 0\right).$$

Using the same argument as that used in the previous proof (kinematic case) and the assumption that $v_t > 0$ proves the convergence of the system to the path. ■

C. Computation of the Control

The previous control U_{dyn} guarantees the asymptotic convergence to the path. Nevertheless, the terms appearing in (15) are not trivially computable. In particular, the computation of $\ddot{\beta}$ refers to the evaluation of jerks $\dddot{u}$ and $\dddot{v}$ through

$$\ddot{\beta} = \frac{1}{v_t^2}(\dddot{v}u - \dddot{u}v) - 2\frac{\dot{v}_t}{v_t}\dot{\beta}. \tag{17}$$

Because it is not realistic to have any measurement of these quantities, the only solution is to rely on a derivation of the dynamic model such that

$$\begin{cases} \dddot{u} = \dfrac{1}{m_u}(\ddot{F} - \ddot{d}_u) \\ \dddot{v} = \dfrac{1}{m_v}(-m_{ur}\ddot{u}r - m_{ur}u\ddot{r} - \ddot{d}_v). \end{cases} \tag{18}$$

This emphasizes the assumption made regarding the neglected dynamics of the system. Then, $\dot{r}$ is rewritten

$$\dot{r} = \frac{f_{\dot{r}_d} - K_3(r - r_d) - K_5(\theta - \delta)}{1 - \dfrac{m_{ur}}{m_v}(\cos\beta)^2}$$

where

$$\begin{aligned} f_{\dot{r}_d} = \dddot{\delta} - K_1(\ddot{\theta} - \ddot{\delta}) + c_c\dddot{s} + g_c\ddot{s} + \frac{\dddot{u}v}{v_t^2} \\ + \frac{2\dot{v}_t\ddot{\beta}}{v_t} + \frac{u}{v_t^2}\left(\frac{m_{ur}}{m_v}\ddot{u}r + \frac{\ddot{d}_v}{m_v}\right). \end{aligned}$$

Then, the control is computed as

$$\Gamma = m_r\dot{r} + d_r.$$

For this expression to be well posed, it must be derived from the robot design parameter

$$\frac{m_{ur}}{m_v} = \frac{m - Y_r}{m - Y_{\dot{v}}}.$$

Analyzing the signs of the hydrodynamic parameters as in [1], we know the following:

- $Y_{\dot{v}}$ is always negative;
- Y_r is positive if stern dominates;
- Y_r is negative if bow dominates.

Thus, in the case of a stern dominant vehicle, the control computation is well posed. For a bow dominant vehicle, the sign of $m - Y_r$ should be taken into account.

D. Robust Control

This section addresses the question of robustness to parameter uncertainties. The previous dynamic control is modified to relax the constraint of having a precise estimation of the dynamic parameters by resorting to backstepping Lyapunov-based techniques.

Recall that the design of the kinematic reference requires an estimation of surge and sway acceleration, relying on the dynamic model, so the errors due to parameters misestimation should explicitly be taken into account in the elaboration of the kinematic reference.

1) Kinematic Reference: In Section III-A, we designed a kinematic reference (13) that includes the computation of $\dot{\beta}$, which can be rewritten as

$$\dot{\beta} = -\sum_{i=1}^{2} q_i g_i - q_3 g_3 r + \dot{u}\frac{v}{v_t^2}.$$

The expression of functions g_i and parameters q_i is displayed in the Appendix. Because r explicitly appears in the previous relation, a proper expression of the kinematic reference is extracted by solving (13) for r, and naming r as r_d, the kinematic reference

$$r_d = \frac{f_r + \sum_{i=1}^{2} q_i g_i - \dot{u}\dfrac{v}{v_t^2}}{1 - q_3 g_3} \tag{19}$$

with $f_r = \dot{\delta} - K_1(\theta - \delta) + c_c(s)\dot{s}$. It should be explicitly established that the resulting expression is well posed in the function of the value of q_3, as mentioned for the dynamic case in Section III-B. This question will be addressed at the dynamic level.

The optimal value for r_d is computed with the real value of parameters q_i^{Re} and a perfect estimation of the forward acceleration $\dot{u}^{\mathrm{Opt}}$. Then, the use of estimated values q_i of the dynamic parameters induces an error such that

$$\Delta r = \frac{\sum_{i=1}^{2} \Delta q_i g_i - \Delta\dot{u}\dfrac{v}{v_t^2} + \Delta q_3 g_3 r}{1 - q_3^{\mathrm{Re}} g_3}$$

with $\Delta q_i = q_i^{\mathrm{Re}} - q_i$ $(i = 1,2,3)$, $\Delta\dot{u} = \dot{u}^{\mathrm{Opt}} - \dot{u}$, and $\Delta r = r^{\mathrm{Opt}} - r$.

Consider the Lyapunov candidate $V_1 = (1/2)(\theta - \delta)^2$. The misestimation of the parameters induces a nonnegative derivative $\dot{V}_1$

$$\dot{V}_1 = -K_1(\theta - \delta)^2 + (\theta - \delta)\Delta r.$$

Because $\dot{V}_1$ is not negative definite, we cannot conclude any convergence property, since the effects of the parameter misestimation still appear in the Lyapunov candidate. Nevertheless, these effects will be canceled at the dynamic level, and asymptotic convergence will be guaranteed. Consider the suboptimal kinematic control (19) as a reference to drive the dynamic controller

$$\tilde{r}_d = \frac{f_r + \sum_{i=1}^{2} q_i g_i - \dot{u}\dfrac{v}{v_t^2}}{1 - q_3 g_3} \tag{20}$$

given q_i, an estimation of q_i^{Re} $(i = 1,2,3)$.

2) Robust Dynamic Control: To deal with robustness to parameter uncertainty, it is necessary to expand the dynamic control expression (16) to make the parameters explicitly appear in the equations, and study the incidence of their misestimation. Considering the previous suboptimal kinematic control as a reference $\tilde{r}_d$ (20), we derive the dynamic control as in Section III-B, explicitly extracting the dynamic parameters

$$\begin{aligned}\tilde{\Gamma} = m_r\left(\dot{\tilde{r}}_d - K_3(r - \tilde{r}_d) - K_5(\theta - \delta)\right)\\ - m_{uv}uv - N_r r - N_{r|r|}r|r|\end{aligned}$$

with

$$\dot{\tilde{r}}_d = R_0^{\dot{r}_d} + \dot{v}R_{\dot{v}}^{\dot{r}_d} + \dot{u}R_{\dot{u}}^{\dot{r}_d} + \ddot{u}R_{\ddot{u}}^{\dot{r}_d} + \dot{u}^2 R_{\dot{u}^2}^{\dot{r}_d} + \dot{u}\dot{v}R_{\dot{u}\dot{v}}^{\dot{r}_d}$$

where $R_0^{\dot{r}_d}, R_{\dot{v}}^{\dot{r}_d}, R_{\dot{u}}^{\dot{r}_d}, R_{\ddot{u}}^{\dot{r}_d}, R_{\dot{u}^2}^{\dot{r}_d}, R_{\dot{u}\dot{v}}^{\dot{r}_d}$ are computable functions dependent on the measurements, listed in the Appendix. Then, $\tilde{\Gamma}$ is rewritten as

$$\begin{aligned}\tilde{\Gamma} = {} & m_r\left(R_0^{\dot{r}_d} - K_3(r - \tilde{r}_d) - K_5(\theta - \delta)\right)\\ & - m_{uv}uv - N_r r - N_{r|r|}r|r| + m_r\dot{v}R_{\dot{v}}^{\dot{r}_d}\\ & + m_r\left(\dot{u}R_{\dot{u}}^{\dot{r}_d} + \ddot{u}R_{\ddot{u}}^{\dot{r}_d} + \dot{u}^2 R_{\dot{u}^2}^{\dot{r}_d} + \dot{u}\dot{v}R_{\dot{u}\dot{v}}^{\dot{r}_d}\right).\end{aligned} \tag{21}$$

Consider now the following version of the control $\tilde{\tilde{\Gamma}}$:

$$\begin{aligned}\tilde{\tilde{\Gamma}} = {} & m_r(R_0^{\dot{r}_d} - K_3(r - \tilde{r}_d) - K_5(\theta - \delta))\\ & - m_{uv}uv - N_r r - N_{r|r|}r|r| + m_r\dot{v}R_{\dot{v}}^{\dot{r}_d}.\end{aligned} \tag{22}$$

Hence, a misestimation of the robot parameters yields a computed control that differs from its optimal version by

$$\begin{aligned}\Delta\tilde{\tilde{\Gamma}} = {} & \Delta[m_r]\left(R_0^{\dot{r}_d} - K_3(r - \tilde{r}_d) - K_5(\theta - \delta)\right)\\ & - \Delta[m_{uv}]uv - \Delta[N_r]r - \Delta[N_{r|r|}]r|r| + \Delta[m_r\dot{v}]R_{\dot{v}}^{\dot{r}_d}\\ & + m_r^{\mathrm{Re}}\dot{u}^{\mathrm{Opt}}\dot{v}^{\mathrm{Opt}}R_{\dot{u}\dot{v}}^{\dot{r}_d}\\ & + m_r^{\mathrm{Re}}\left(\dot{u}^{\mathrm{Opt}}R_{\dot{u}}^{\dot{r}_d} + \ddot{u}^{\mathrm{Opt}}R_{\ddot{u}}^{\dot{r}_d} + (\dot{u}^{\mathrm{Opt}})^2 R_{\dot{u}^2}^{\dot{r}_d}\right)\end{aligned}$$

with $\Delta[m_r\dot{v}] = m_r^{\mathrm{Re}}\dot{v}^{\mathrm{Opt}} - m_r\dot{v}$, and so on. Using the expression of $\dot{v}$, extracted form (4), $\Delta\tilde{\tilde{\Gamma}}$ is rewritten as

$$\Delta\tilde{\tilde{\Gamma}} = \sum_{i=1}^{7}\Delta p_i f_i + \Phi(.)$$

where $\Phi(.) = m_r^{\mathrm{Re}}\dot{u}^{\mathrm{Opt}}\dot{v}^{\mathrm{Opt}}R_{\dot{u}\dot{v}}^{\dot{r}_d} + m_r^{\mathrm{Re}}(\dot{u}^{\mathrm{Opt}}R_{\dot{u}}^{\dot{r}_d} + \ddot{u}^{\mathrm{Opt}}R_{\ddot{u}}^{\dot{r}_d} + (\dot{u}^{\mathrm{Opt}})^2 R_{\dot{u}^2}^{\dot{r}_d})$. The parameters p_i and the functions f_i are listed in the Appendix.

Consider the following Lyapunov candidate that captures the system's property of convergence to the suboptimal reference $\tilde{r}_d$:

$$V_6 = \frac{1}{2}(r - \tilde{r}_d)^2 + \frac{1}{2}\sum_{i=1}^{7}\frac{(\Delta p_i)^2}{\lambda_i^p}$$

and, with control (21) and parameter adaptation scheme

$$\dot{p}_i = -\lambda_i^p(r - \tilde{r}_d)f_i, \qquad i = 1\ldots 7 \tag{23}$$

yields the following derivative:

$$\dot{V}_6 = -K_3(r - \tilde{r}_d)^2 + (r - \tilde{r}_d)\Phi(.).$$

Consider now the forward control, and expand (16)

$$F = \sum_{i=1}^{4} d_i l_i. \tag{24}$$

The parameters d_i and the functions l_i are listed in the Appendix. The misestimation $\Delta d_i = d_i^{\mathrm{Re}} - d_i$, for $i = 1,2,3,4$,

induces a computed forward control different from the optimal one such that

$$\Delta F = F^{\mathrm{Opt}} - F = \sum_{i=1}^{4} \Delta d_i l_i.$$

Then, considering the following Lyapunov candidate:

$$V_5 = \frac{1}{2}(u-u_d)^2 + \frac{1}{2}\sum_{i=1}^{4}\frac{\Delta d_i l_i}{\lambda_i^d}$$

with control (24) and the following parameter adaptation scheme:

$$\dot{d}_i = -\lambda_i^d (u-u_d) l_i, \qquad i = 1\ldots 4 \tag{25}$$

leads to a negative–definite derivative

$$\dot{V}_5 = -K_5(u-u_d)^2 \leq 0.$$

Then, noting that $\ddot{V}_5$ is bounded, the use of the CBL proves the asymptotic convergence of u to u_d. Hence, $\dot{u}$ and $\ddot{u}$ vanish with time

$$\lim_{t\to\infty} \dot{u} = 0$$
$$\lim_{t\to\infty} \ddot{u} = 0.$$

The previous argument implies that the system will asymptotically reach the invariant set

$$\Omega^{\dot{u}} = [x, y, \theta, u, v, r, s | \dot{u} = 0, \ddot{u} = 0]. \tag{26}$$

Studying the system trajectories onto the $\Omega^{\dot{u}}$ set, we notice that

$$\Phi(.)|_{\Omega^{\dot{u}}} = 0$$

hence

$$\dot{V}_6|_{\Omega^{\dot{u}}} = -K_3(r-\tilde{r}_d)^2 \leq 0.$$

Noting that $\ddot{V}_6$ is bounded, and using the invariance principle, the previous arguments imply

$$\lim_{t\to\infty} r = \tilde{r}_d.$$

Then, the system will asymptotically reach the invariant set $\Omega^{\tilde{r}_d} \subset \Omega^{\dot{u}}$ defined as

$$\Omega^{\tilde{r}_d} = [x, y, \theta, u, v, r, s | r = \tilde{r}_d]. \tag{27}$$

The system trajectories onto this set are described by the $V_1|_{\Omega^{\tilde{r}_d}}$ Lyapunov candidate. In this set, the derivative is written as

$$\dot{V}_1|_{\Omega^{\tilde{r}_d}} = \frac{(\theta-\delta)}{1-q_3^{\mathrm{Re}} g_3}\left(\sum_{i=1}^{2}\Delta q_i g_i + \Delta q_3 g_3 r\right) - K_1(\theta-\delta)^2.$$

The effects of the misestimation of parameter q_i are still present, and we do not consider the previously used solution of adapting its estimation since the knowledge of q_3^{Re} is required to design a classic adaptive scheme.

The proposed solution consists in relying on switching control system theory to guarantee that $\dot{V}_1$ is negative definite. For more information on switching control systems, please refer to [27] and [32]. To insure asymptotic convergence, one should insure that

$$\frac{(\theta-\delta)}{1-q_3^{\mathrm{Re}} g_3}\left(\sum_{i=1}^{2}\Delta q_i g_i + \Delta q_3 g_3 r\right) \leq 0 \qquad \forall t.$$

This can be done by choosing two different values q_i^{up} and q_i^{down}, guaranteed to overestimate and underestimate the real value q_i^{Re} ($\Delta q_i^{\mathrm{up}} > 0$ and $\Delta q_i^{\mathrm{down}} < 0$), and use them such that

$$q_i = \begin{cases} q_i^{\mathrm{up}}, & \text{if } (\theta-\delta) g_i < 0 \\ q_i^{\mathrm{down}}, & \text{if } (\theta-\delta) g_i > 0 \end{cases}$$
$$q_3 = \begin{cases} q_3^{\mathrm{up}}, & \text{if } (\theta-\delta) r < 0 \\ q_3^{\mathrm{down}}, & \text{if } (\theta-\delta) r > 0 \end{cases} \tag{28}$$

using the facts that $g_3 > 0$ and $(1 - q_3 g_3) > 0, \forall t$. Then, using (28) switching conditions, we conclude that $\dot{V}_1|_{\Omega^{\dot{u}}} < 0$.

Because eight possible Lyapunov functions are negative definite, and the switching process does not affect the convergence [27], we can state that

$$\lim_{t\to\infty} \theta = \delta|_{t\to\infty}.$$

Using the same argument concerning the imbricated invariant set, it has been shown that the robot asymptotically converges to the path. We are now able to state Proposition 3 that solves problem $\mathbf{C_3}$.

Proposition 3: Consider the robot models (3) and (4) and the desired approach angle defined in (6), where k_δ is a positive gain and $0 < \theta_a < \pi/2$. Further, assume that measurements of $[u\ v\ r]^T$ are available from robot sensors and that a parameterization of the path is available such that, given s, the curvilinear abscissa of a point on the path, the variables $\theta, x_{B/F}, y_{B/F}, c_c, (\partial c_c/\partial s)$ are well defined and computable. Consider that a reasonable estimation of the model parameters $\tilde{m}_u, \tilde{m}_v, \tilde{m}_r, \tilde{m}_{uv}, \tilde{X}_u, \tilde{X}_{u|u|}, \tilde{Y}_v, \tilde{Y}_{v|v|}, \tilde{N}_r, \tilde{N}_{r|r|}$ was used to compute the 11 initial values p_i^0, d_j^0 $(i = 1\ldots 7, j = 1\ldots 4)$ as described in the tables of the Appendix, and q_k^{up} and q_k^{down} such that $q_k^{\mathrm{up}} > q_k^{\mathrm{Re}} > q_k^{\mathrm{down}}$, $(k = 1\ldots 3)$. Define u_d as the desired forward velocity. Then, the control law

$$U_{\mathrm{dyn}}^{\mathrm{Rbst}} = \begin{cases} \Gamma = \sum_{i=1}^{7} p_i f_i \\ F = \sum_{j=1}^{4} d_j l_j \end{cases} \tag{29}$$

with the kinematic reference

$$\tilde{r}_d = \frac{1}{1-q_3 g_3}\left(\dot{\delta} - K_1(\theta-\delta) + c_c(s)\dot{s} - (\dot{u}_d - K_5(u-u_d))\frac{v}{v_t^2} + \sum_{k=1}^{2} q_k g_k\right)$$
$$\dot{s} = v_t \cos\theta + K_2 x_{B/F}$$

the adaptation scheme (23), (25) and the switching scheme (28), with $\lambda_i^p, \lambda_j^d, K_1, K_2, K_3, K_4, K_5$ positive gains, the assumption that $v_t > 0, \forall t$, and given the initial relative position $[\theta, x_{B/F}, y_{B/F}]|_{t=0}$, solves problem $\mathbf{C_3}$.

TABLE I
PATH PARAMETERS

$a_0 = 0\, a_1 = 0.866\, a_2 = -0.02\, a_3 = 10^{-5}\, a_4 = 1.5.10^{-6}$
$b_0 = 0\, b_1 = 0.5\, b_2 = -5.10^{-4}\, b_3 = 10^{-5}\, b_4 = 10^{-7}$

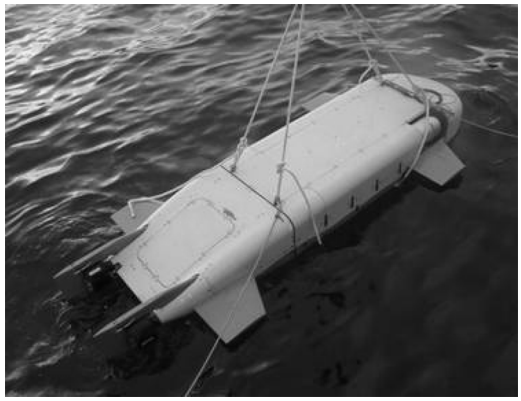

Fig. 2. Infante AUV (IST) during its first sea trial.

Note that the evolution of the parameters is a function of the excitation of the problem. Analyzing the adaptation equations, it is easy to see that the adaptation stops when the reference errors $(r - r_d)$ and $(\theta - \delta)$ are equal to zero. This phenomenon is easily observed for linear systems when the path does not lead to sufficient excitation, and in this case, the estimated value of the parameters does not converge to the real value [31], [38].

Another solution, based on switching system theory, is imaginable. It consists in developing a switching scheme for all parameters, as for the q_i parameters. Further research on this topic is warranted.

IV. SIMULATION RESULTS

The aim of the simulation is to illustrate the efficiency of the previous controllers in driving an AUV onto a desired path. The path is characterized by a curvature c_c on a point F, parameterized by its curvilinear abscissa s. The objective is to regulate the distance to the path and the heading of the total velocity of the robot to zero relative to the given path. To test these controllers in a general case, we have chosen to consider the more complex path defined in Section IV-A.

A. Path Parameterization

The path is designed in Cartesian space (cf., Table I) and we assume to have a parameterization that allows the computation of the following items (given s):

- $\Psi_{F/0}(s)$: the global heading of the virtual target;
- $c_c(s)$: the path curvature at the target position;
- $\partial c_c(s)/\partial s$: the curvilinear derivative of the curvature at the target position;
- $x_{F/0}$ and $y_{F/0}$, the absolute location of the virtual target.

We have chosen a polynomial parameterization of the form

$$x_{F/0}(\mu) = \sum_{i=0}^{n} a_i \mu^i, \quad y_{F/0}(\mu) = \sum_{i=0}^{n} b_i \mu^i.$$

TABLE II
PARAMETERS OF THE SIMPLIFIED MODEL OF THE INFANTE AUV (IST) ***[AU: Please add space between unit and number; please change a period between units to a \cdot and please use regular font, not italics to present units]***

$m = 2234Kg$	$I_z = 2000N.m.s^2$
$X_{\dot{u}} = -142Kg.$	$Y_{\dot{v}} = -1715Kg.$
$N_{\dot{r}} = -1349N.m.s^2$	$X_u = 0Kg.m^{-1}$
$Y_v = -346Kg.m^{-1}$	$N_r = -1427N.m.s.$
$X_{u\|u\|} = -35Kg.m^{-1}$	$Y_v\|v\| = -667Kg.s^{-1}$
$N_r\|r\| = -310N.m.s.$	

TABLE III
DYNAMIC CONTROL PARAMETERS

$K_1 = 1$	$K_2 = 1$	$K_3 = 1$	$K_4 = 1$	$K_5 = 1$
$K_\delta = 1$	$\theta_a = \pi/4$	$u_d = 2$	$\dot{u}_d = 0$	$\ddot{u}_d = 0$

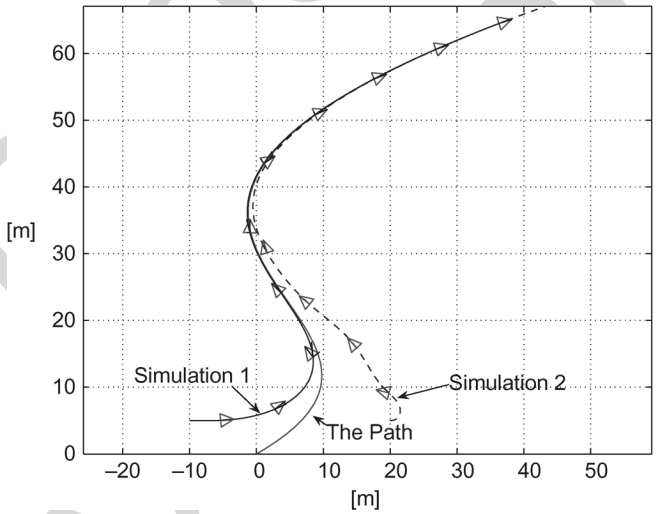

Fig. 3. System trajectories, when considering a perfect knowledge of the parameters (simulation 1: solid line; simulation 2: dashed line).

Assuming we have a precise estimation of function $\mu(s)$, and given s, we compute

$$\begin{aligned}
\Psi_{F/0}(s) &= \arctan \frac{(y_{F/0})'}{(x_{F/0})'} \\
c_c(s) &= \frac{\partial \Psi_{F/0}(s)}{\partial \mu} \frac{d\mu}{ds} \\
\frac{\partial c_c(s)}{\partial s} &= \frac{\partial c_c(s)}{\partial \mu} \frac{d\mu}{ds} \\
x_{F/0}(\mu(s)) \quad ; & \quad y_{F/0}(\mu(s)) \\
(x_{F/0})' = \frac{dx_{F/0}}{d\mu} \quad ; & \quad (y_{F/0})' = \frac{dy_{F/0}}{d\mu}.
\end{aligned}$$

The estimation of function $\mu(s)$ is achieved by integration of

$$\frac{d\mu}{ds} = \frac{1}{\sqrt{\left[(x_{F/0})'\right]^2 + \left[(y_{F/0})'\right]^2}}.$$

The model of the robot is a simplified version of Infante [36], the AUV developed at the DSOR (Fig. 2), given in Table II.

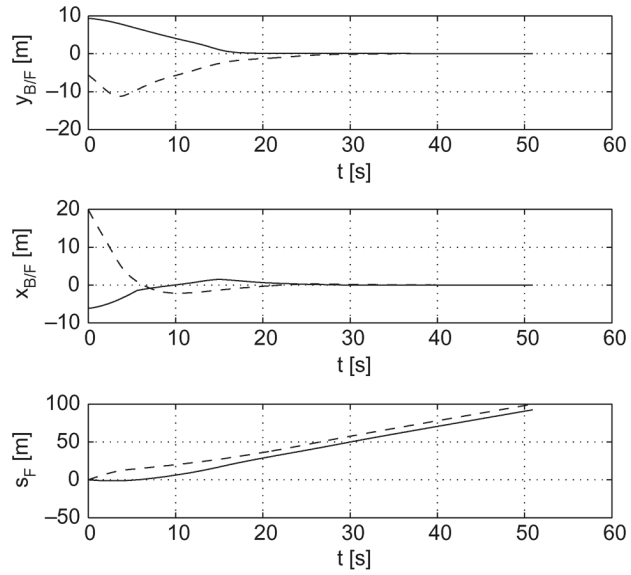

Fig. 4. Relative distance robot/rabit evolution, when considering a perfect knowledge of the parameters (simulation 1: solid line; simulation 2: dashed line).

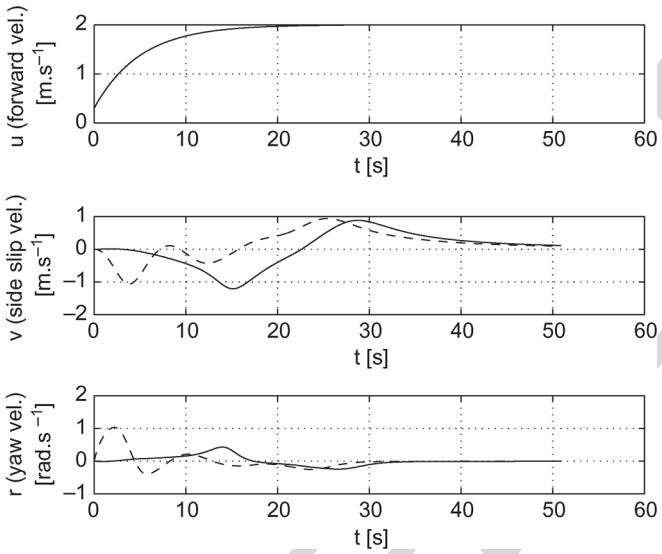

Fig. 5. System velocities evolution, when considering a perfect knowledge of the parameters (simulation 1: solid line; simulation 2: dashed line).

B. Dynamic Controller

The simulations are carried out using the robot parameters of Table II, the control parameters of Table III, and the path parameters of Table I.

The simulation results are displayed in Figs. 3–6.

Discussion: Both simulation results of Fig. 3 show a satisfactory behavior of the AUV, clearly driven to reach and stay on the path. Fig. 4 indicates the evolution of the relative distance between the virtual target and the robot, expressed in the Serret–Frenet frame. The concurrent convergence of $x_{B/F}$ and $y_{B/F}$ to zero confirms the desired behavior of the system. Note that since $x_{B/F}$ converges to zero, the virtual target converges to the closest point on the path. Figs. 5 and 6 show the system velocities' evolution and the related control activity. Concerning

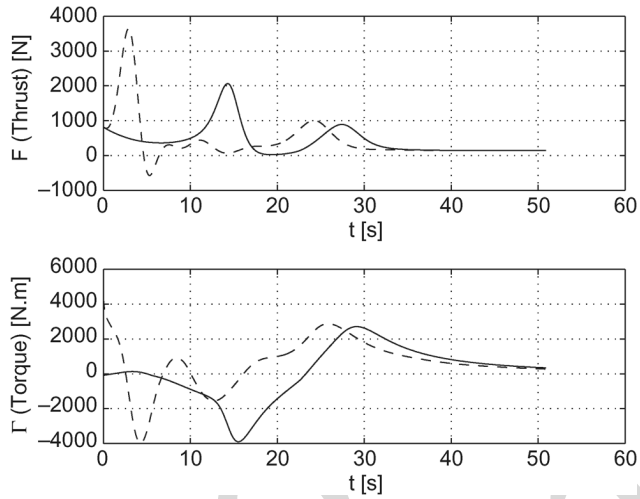

Fig. 6. Control activity, when considering a perfect knowledge of the parameters (simulation 1: solid line; simulation 2: dashed line).

TABLE IV
INITIAL PARAMETERS ESTIMATION *[AU; Please follow the request in Table II]*

$m = 3000Kg$	$I_z = 1000N.m.s^2$
$X_{\dot{u}} = -10Kg.$	$Y_{\dot{v}} = -2500Kg.$
$N_{\dot{r}} = -500N.m.s^2$	$X_u = -10Kg.s^{-1}$
$Y_v = -500Kg.s^{-1}$	$N_r = -500N.m.s.$
$X_{u\|u\|} = -10Kg.m^{-1}$	$Y_v\|v\| = -100Kg.s^{-1}$
$N_r\|r\| = -100N.m.s.$	

the amplitude of the control activity, recall that the simulated system is heavy (cf., Table II). Note that the tunable parameters of the proposed control are the control gains K_i, $i = 1, 2, 3, 4$, and the guidance parameters, the asymptotic approach angle, denoted θ_a, and the gain k_δ, designing the smoothness of this approach.

C. Robust Controller

To demonstrate the efficiency of the robust scheme, we first proceed to simulations considering the misestimated parameters of Table IV, without adaptation. The results are given in Figs. 7–10 (dotted lines).

The robust scheme is tested using the path parameters of Table I and the control parameters of Table III. The system parameter estimated values are displayed in Table IV, used to compute the 11 initial values of the parameter groups. The surrounding values for q_1, q_2, and q_4 parameter groups are also considered. The expression of the parameter groups is listed in the Appendix

$$q_1^{\text{up}} = -0.1051, \quad q_1^{\text{down}} = -0.0526$$
$$q_2^{\text{up}} = -0.2534, \quad q_2^{\text{down}} = -0.0676$$
$$q_3^{\text{up}} = 0.5, \quad q_3^{\text{down}} = 0.7.$$

The results are displayed in Figs. 7–10 (straight lines). The adaptation evolution for parameters p_j, $j = 1 \ldots 7$, is given in Figs. 11 and 12, q_i, $i = 1, 2, 3$ in Fig. 13, and d_k, $k = 1 \ldots 4$, in Fig. 14. The convergence gains have been tuned according to

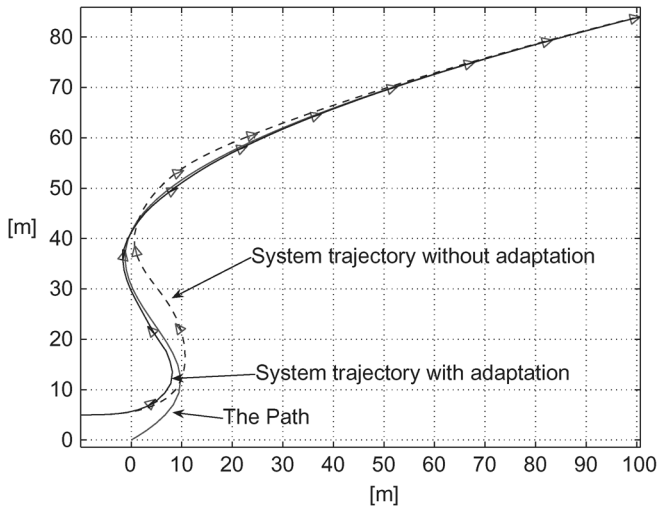

Fig. 7. System trajectories using robust control (solid line) and dynamic control with misestimated parameters (dotted line).

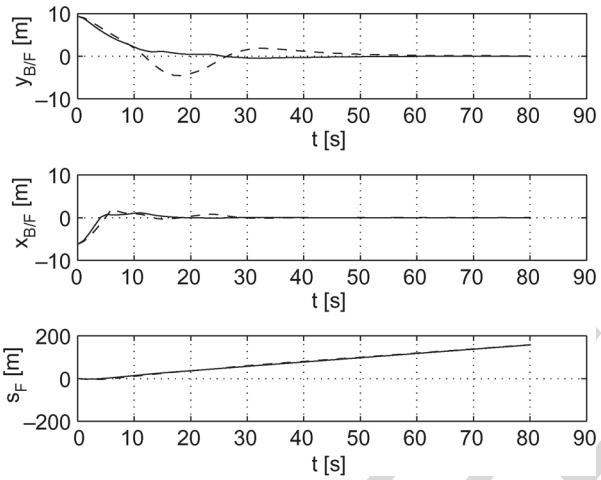

Fig. 8. Relative distance robot/rabit evolution using robust control (solid line) and dynamic control with misestimated parameters (dashed line).

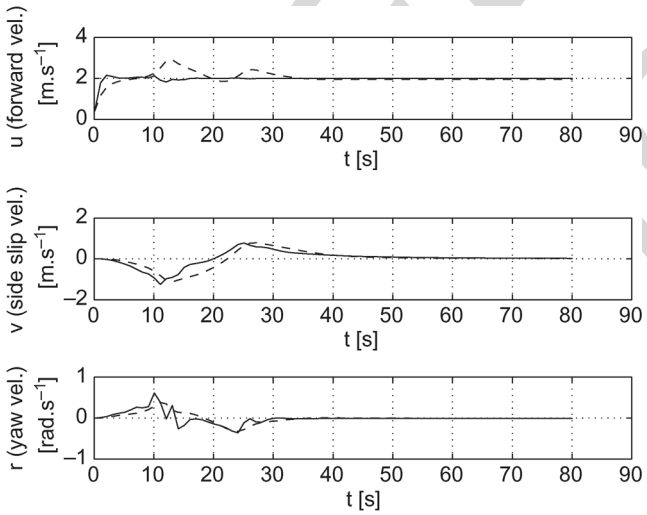

Fig. 9. Velocities evolution using robust control (solid line) and dynamic control with misestimated parameters (dashed line).

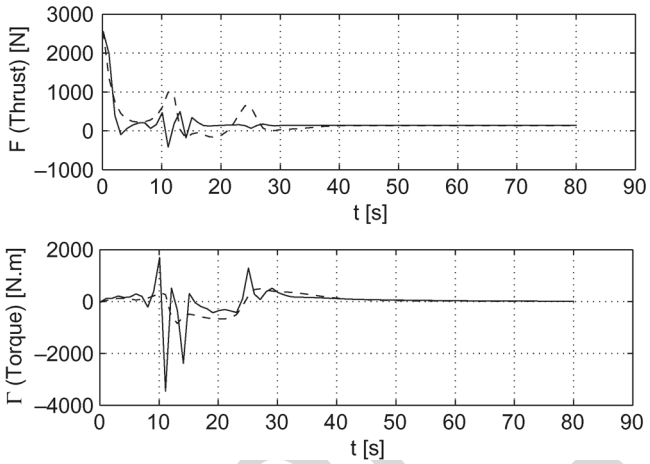

Fig. 10. Control activity, using robust control (solid line) and dynamic control with misestimated parameters (dashed line).

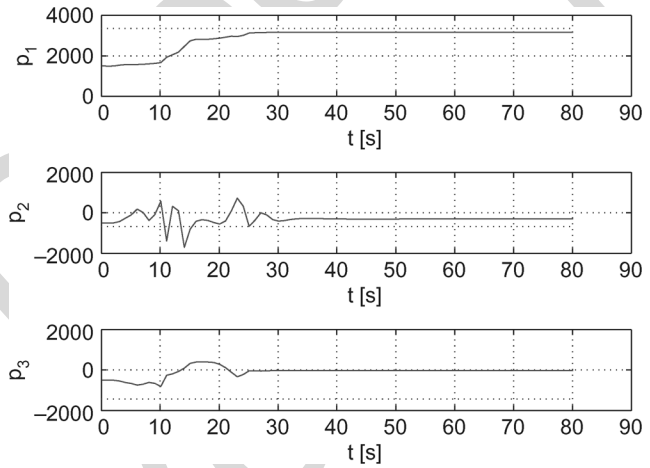

Fig. 11. Evolution of the adaptation of parameters p_i $(i = 1, 2, 3)$ involved in the computation of Γ.

Table V, to observe the convergence of the parameters during the simulation.

Discussion: Trajectories of Fig. 7 clearly indicate the improvement of the robust control with respect to the performances of the dynamic control with misestimated parameters. Note that since the desired path is getting flatter the convergence of the dynamic control is achieved much more later than the robust control results. This compared analysis is confirmed by the evolution of the relative distance between the virtual target and the robot, displayed in Fig. 8, where the convergence evolution of the $y_{B/F}$ variable is similar to the one in the case of a perfect knowledge of the parameters (cf., Fig. 4), which is clearly not the case of the response considering misestimated parameters, without the robust scheme. Fig. 9 indicates also a better convergence of the forward velocity u to the desired one $u_d = 2\ \mathrm{m.s}^{-1}$, when using the robust control. Fig. 10 displays the evolution of the control activity evolution with and without the robust scheme. As expected, the control activity is higher with the robust control. Moreover, the control activity profile of the robust control (solid line) presents some important discontinuities, induced by the switching part of the robust scheme, as one could have expected. The reduction of this chattering effect

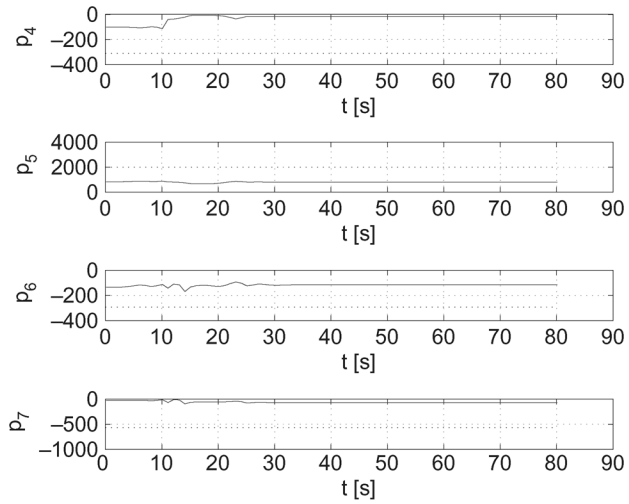

Fig. 12. Evolution of the adaptation of parameters p_i $(i = 4, 5, 6, 7)$ involved in the computation of Γ.

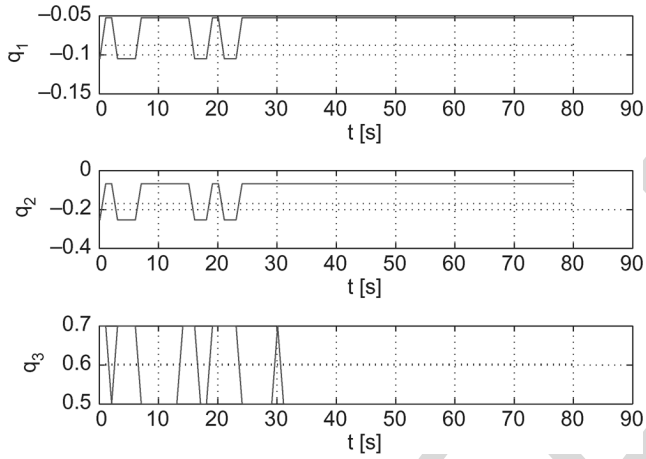

Fig. 13. Evolution of the commutations of parameters involved in the computation of the kinematic reference r_d.

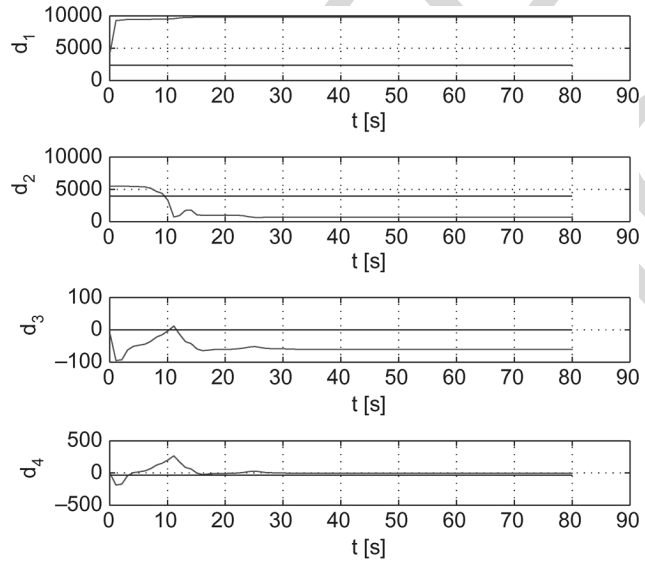

Fig. 14. Evolution of the adaptation of parameters involved in the computation of F.

TABLE V
CONVERGENCE GAINS OF THE ADAPTATION SCHEME

$\lambda_1^p = 30$	$\lambda_2^p = 50$	$\lambda_3^p = 50$	$\lambda_4^p = 10$
$\lambda_5^p = 10$	$\lambda_6^p = 5$	$\lambda_7^p = 8$	$\lambda_1^d = 100$
$\lambda_2^d = 500$	$\lambda_3^d = 1$	$\lambda_4^d = 2$	

TABLE VI
KINEMATIC REFERENCE PARAMETER GROUPS AND FUNCTIONS

q_1 and g_1	q_2 and g_2	q_3 and g_3
$\frac{Y_v}{m_v}$	$\frac{Y_{v\|v\|}}{m_v}$	$\frac{m_{ur}}{m_v}$
$\frac{uv}{v_t^2}$	$\frac{uv\|v\|}{v_t^2}$	$\frac{u^2}{v_t^2}$

TABLE VII
FORWARD CONTROL PARAMETER GROUPS AND FUNCTIONS

d_1 and l_1	d_2 and l_2
m_u	m_{uv}
$\dot{u}_d - K_5(u - u_d)$	$-vr$
d_3 and l_3	d_4 and l_4
X_u	$X_{u\|u\|}$
$-u$	$-u\|u\|$

TABLE VIII
HEADING CONTROL PARAMETER GROUPS AND FUNCTIONS

p_1 and f_1	p_2 and f_2	p_3 and f_3
m_r	$\frac{m_{ur}m_r}{m_v}$	$\frac{Y_v m_r}{m_v}$
$R_0^{\dot{r}_d} - K_3(r - \tilde{r}_d) - K_5(\theta - \delta)$	$-urR_{\dot{v}}^{\dot{r}_d}$	$vR_{\dot{v}}^{\dot{r}_d}$
p_4 and f_4	p_5 and f_5	p_6 and f_6
$\frac{Y_{v\|v\|}m_r}{m_v}$	m_{uv}	N_r
$v\|v\|R_{\dot{v}}^{\dot{r}_d}$	$-uv$	$-r$
p_7 and f_7		
$N_{r\|r\|}$		
$-r\|r\|$		

could be a substantial improvement of the method. Figs. 11 and 11***[AU: Should it be "Figs. 11 and 12"?]*** show the evolution of parameters p_i, $i = 1, \ldots, 7$, involved in the computation of Γ. It could be noted that the parameters are not converging to their real value. This is expected since the related Lyapunov functions (cf., Section III-D2) that warrants the convergence guaranties of the tracking variables, do not consider the convergence of the parameters to their actual value. This is a known behavior of adaptive control, that is, for the linear case, a problem of excitation of the system. This robust control is not designed to make the parameters estimation, but to desensitize the system properties to the parameters misestimation. Fig. 13 shows the evolution of the parameters involved in the computation of the kinematic reference r_d, according to the designed switching scheme. Note that one of the assumption of the problem is that the system is able to switch infinitively fast, and further research on this topic will include the dwell time property of the system, to establish the practical convergence performance of the method. Indeed, including a realistic dwell time in the study will make it impossible to meet asymptotic convergence property, and only practical convergence will be reachable.

TABLE IX
ELEMENTS OF COMPUTATION OF PARAMETER GROUPS AND FUNCTIONS

$R_0^{\dot{r}_d} = f_0^{r_d}(g_1^0 + g_2^0 + g_3^0)$
$R_{\dot{v}}^{\dot{r}_d} = g_0^{\dot{v}} f_1^{r_d} + f_0^{r_d}(g_1^{\dot{v}} + g_2^{\dot{v}} + g_3^{\dot{v}} + g_4^{\dot{v}} + g_5^{\dot{v}})$
$R_{\dot{u}}^{\dot{r}_d} = g_0^{\dot{u}} f_1^{r_d} + f_0^{r_d}(g_1^{\dot{u}} + g_2^{\dot{u}} + g_3^{\dot{u}} + g_4^{\dot{u}} + g_5^{\dot{u}})$
$R_{\ddot{u}}^{\dot{r}_d} = f_0^{r_d} g_1^{\ddot{u}}$
$R_{\dot{u}.\dot{u}}^{\dot{r}_d} = f_0^{r_d} g_1^{\dot{u}.\dot{u}} + g_0^{\dot{u}} g_1^{\ddot{u}}$
$R_{\dot{u}.\dot{v}}^{\dot{r}_d} = f_0^{r_d} g_1^{\dot{u}.\dot{v}} + g_0^{\dot{v}} g_1^{\ddot{u}}$

TABLE X
ELEMENTS OF COMPUTATION OF PARAMETER GROUPS AND FUNCTIONS

$f_0^{r_d}$	$=$	$\frac{1}{1-q_3\frac{u^2}{v_t^2}}$
$f_1^{r_d}$	$=$	$f_r + \sum_{i=1}^{2} q_i g_i$
g_1^0	$=$	$\frac{\partial^2\dot{\delta}}{\partial y^2}\dot{y}^2 + \frac{\partial\dot{\delta}}{\partial y}(-\frac{\partial c_c}{\partial s}\dot{s}^2$ $-c_c\dot{x}\dot{s} + v_t\cos\theta(r - c_c\dot{s})$ $-c_c x K_2\dot{x} + c_c x\sin\theta v_t(r - c_c\dot{s}))$
g_2^0	$=$	$K_1(\dot{\delta} - (r - c_c\dot{s}))$
g_3^0	$=$	$\frac{\partial c_c}{\partial s}\dot{s}^2 + c_c(K_2\dot{x} - \sin\theta v_t(r - c_c\dot{s}))$
$g_0^{\dot{v}}$	$=$	$\frac{q_3}{(1-q_3 g_3)^2}(-\frac{2u^2 v}{v_t^4})$
$g_0^{\dot{u}}$	$=$	$\frac{q_3}{(1-q_3 g_3)^2}(\frac{2uv^2}{v_t^4})$
$g_1^{\dot{v}}$	$=$	$\frac{\partial\dot{\delta}}{\partial y}\frac{1}{v_t}(\sin\theta v + \cos\theta u$ $-c_c x(\cos\theta v - \sin\theta u))$
$g_1^{\dot{u}}$	$=$	$\frac{\partial\dot{\delta}}{\partial y}\frac{1}{v_t}(\sin\theta u - \cos\theta v$ $-c_c x(\cos\theta u + \sin\theta v))$
$g_2^{\dot{v}}$	$=$	$-K_1\frac{u}{v_t^2}$
$g_2^{\dot{u}}$	$=$	$-K_1\frac{v}{v_t^2}$
$g_3^{\dot{v}}$	$=$	$\frac{c_c}{v_t}(\cos\theta v - \sin\theta u)$
$g_3^{\dot{u}}$	$=$	$\frac{c_c}{v_t}(\cos\theta u + \sin\theta v)$
$g_4^{\dot{v}}$	$=$	$q_1\frac{u(u^2-v^2)}{v_t^4}$
$g_4^{\dot{u}}$	$=$	$q_1\frac{v(v^2-u^2)}{v_t^4}$
$g_5^{\dot{v}}$	$=$	$q_2\frac{2u^3\lvert v\rvert}{v_t^4}$
$g_5^{\dot{u}}$	$=$	$q_2\frac{v\lvert v\rvert(v^2-u^2)}{v_t^4}$
$g_1^{\ddot{u}}$	$=$	$\frac{v}{v_t^2}$
$g_1^{\dot{u}\dot{v}}$	$=$	$\frac{u^2-v^2}{v_t^4}$
$g_1^{\dot{u}\dot{u}}$	$=$	$\frac{-2uv}{v_t^4}$

V. CONCLUSION

We have developed a dynamic robust path-following AUV control that exhibits good performances. The proposed method uses a hybrid robust scheme, relying on classic adaptation scheme design of those dynamic parameters that appear with an affine form, and on switching control for the others. A robot design limitation reduces the application field of this solution to torpedo-shaped vehicles that ensure that the ratio m_u/m_v stays far from 1. The asymptotic convergence of the controlled system is shown in the Lyapunov sense. To complete this study, disturbance rejection and unmodeled dynamic robustness must be explicitly addressed, with the introduction of a dwell time, the shortest switching period of the system. Another approach is now under study, relying exclusively on switching system theory. This warrants further research.

APPENDIX
FUNCTIONS AND PARAMETER GROUPS

In the sequel, we present the expression of the functions and parameter group used in Section III-D.

A. Kinematic Reference

The kinematic references, denoted r_d, is rewritten according to (19), where functions g_i and parameter groups q_i, $i = 1, 2, 3$, have the following expression, displayed in Table VI.

B. Forward Control F

The expression of the forward control, denoted F, is rewritten according to (24), where functions l_i and parameter groups d_i, $i = 1, 2, 3, 4$, are expressed in Table VII.

C. Heading Control Γ

The expression of the torque control, denoted Γ, is rewritten according to (29), where functions f_i and parameter groups p_i, $i = 1, \ldots, 7$, are expressed in Tables VIII–X.

ACKNOWLEDGMENT

The authors would like to thank Prof. A. Pascoal and his team for their helpful comments.

REFERENCES

[1] ***[AU: Please provide the referenced pages]***E. Lewis, *Principles of Naval Architecure—Vol III: Motions in Waves and Controllability*. New York: Society of Naval Architects and Marine Engineers (SNAME), 1989.

[2] L. Ji-Hong and L. Pan-Mook, "Design of an adaptive nonlinear controller for depth control of an autonomous underwater vehicle," *Ocean Eng.*, vol. 32, no. 17–18, pp. 2165–2181, 2005.

[3] T. Prestero, "Verification of a six degree of freedom simulation model for the REMUS autonomous underwater vehicle" M.S. thesis, Ocean Mech. Eng., Massachusetts Inst. Technol./Woods Hole Ocean. Inst., Cambridge, MA, Sep. 2001 [Online]. Available: http://www.mit.edu/tprester/main.pdf

[4] D. Soetanto, L. Lapierre, and A. Pascoal, "Adaptive, non-singular path following control of a wheeled robot," in *Proc. IEEE Conf. Decision Control*, Maui, HI, Dec. 9–12, 2003, pp. 1765–1770.

[5] A. Healey and D. Lienard, "Multivariable sliding mode control for autonomous diving and steering of unmanned underwater vehicles," *IEEE J. Ocean. Eng.*, vol. 18, no. 3, pp. 327–339, Jul. 1993.

[6] L. Lapierre, D. Soetanto, and A. Pascoal, "Non-linear path-following control of an AUV," in *Proc. IEEE Conf. Decision Control*, Maui, HI, Dec. 9–12, 2003, pp. 1256–1261.

[7] M. Krstic, I. Kanellakopoulos, and P. Kokotovic, *Nonlinear and Adaptive Control Design*. New York: Wiley, 1995.

[8] F. Song and S. Smith, "Design of sliding mode fuzzy controllers for an autonomous underwater vehicle without system model," in *Proc. MTS/IEEE OCEANS Conf.*, Providence, RI, Sep. 9–14, 2000, pp. 835–840.

[9] W. Naeem, R. Sutton, and S. Ahmad, "Pure pursuit guidance and model predictive control of an autonomous underwater vehicle for cable/pipeline tracking," *IMarEST J. Mar. Sci. Environ.*, no. 1, pt. C, pp. 15–25, Mar. 2004.

[10] ***[AU: Please define UKACC]***W. Naeem, "Model predictive control of an autonomous underwater vehicle," in *Proc. UKACC Postgraduate Symp.*, Sheffield, U.K., Sep. 2002, pp. 19–23.

[11] T. Salgado-Jmenez, J. Spiewak, P. Fraisse, and B. Jouvencel, "A robust control algorithm for AUV: Based on a high order sliding mode," in *Proc. MTS/IEEE Int. OCEANS. Conf.*, Kobe, Japan, Nov. 9–12, 2004, pp. 276–281.

[12] ***[AU: Please provide the referenced pages]***J. Slotine and W. Li, *Applied Nonlinear Control*. Englewood Cliffs, NJ: Prentice-Hall, 1991.

[13] C. Silvestre, A. Pascoal, and I. Kaminer, "On the design of gain-scheduled trajectory tracking controllers," *Int. J. Robust Nonlinear Control*, vol. 12, no. 9, pp. 797–839, Jul. 2002.

[14] ***[AU: Please provide department]***M. Kim, "Nonlinear control and robust observer design for marine vehicles," Ph.D. dissertation, Virginia Polytech. Inst. State Univ., Blacksburg, VA, Nov. 3, 2000.

[15] ***[AU: Please provide the referenced pages]***T. Fossen, *Guidance and Control of Ocean Vehicles*. New York: Wiley, 1994.

[16] M. Aucher, "Dynamique des sous-marins," Paris, France, Internal Rep., science et technique de l'armement, 55, 4 fasc, 1981.

[17] L. Lapierre, D. Soetanto, and A. Pascoal, "Nonsingular path following control of a unicycle in the presence of parametric modelling uncertainties," *Int. J. Robust Nonlinear Control*, vol. 16, no. 10, pp. 485–503, Apr. 2006.

[18] P. Encarnacao, A. Pascoal, and M. Arcak, "Path following for autonomous marine craft," in *Proc. 5th IFAC Conf. Mar. Craft Maneuver. Control*, Aalborg, Denmark, Aug. 2000, pp. 117–122.

[19] P. Encarnacao, A. Pascoal, and M. Arcak, "Path following for marine vehicle in the presence of unknown currents," in *Proc. 6th IFAC Symp. Robot Control*, Vienna, Austria, Dec. 2000, vol. II, pp. 469–474.

[20] A. Aguiar, A. Atassi, and A. Pascoal, "Regulation of a non-holonomic dynamic wheeled mobile robot with parametric modeling uncertainty using Lyapunov function," in *Proc. 39th IEEE Conf. Decision Control*, Sydney, Australia, Dec. 2000, vol. 3, pp. 2995–3000.

[21] ***[AU: Please define IST/ISR]***A. Aguiar, "Nonlinear motion control of non-holonomic and underactuated systems," Ph.D. dissertation, IST/ISR, Lisbon, Portugal, Apr. 2002.

[22] N. Andreff, B. Espiau, and R. Horaud, "Visual servoing from line," Tech. Rep. INRIA n4226, Jul. 2001 [Online]. Available: http://www.inria.fr/rrrt/rr-4226.html

[23] C. Canudas de Wit, H. Khennouf, and C. Samson, "Non-linear control design for mobile robots," in *Recent Trends in Mobile Robotics*, ser. Robotics and Automated Systems, Y. F. Zheng, Ed. Singapore: World Scientific, vol. 11, pp. 121–156.

[24] ***[AU: Please provide page range]***F. Diaz del Rio, G. Jimenez, J. Sevillano, S. Amaya, and A. Balcells, "A new method for tracking memorized paths: Application to unicycle robots," in *Proc. 10th Mediterranean Conf. Control*, Lisbon, Portugal, Jul. 9–12, 2002.

[25] ***[AU: Please provide referenced pages]***W. E. Dixon, D. M. Dawson, E. Zergeroglu, and A. Behal, "Non linear control of wheeled robots," in *Lecture Notes in Control and Information Sciences*. Berlin, Germany: Springler-Verlag, 2001, vol. 262.

[26] ***[AU: Please define IST/ISR]***P. M. Encarnao, "Non linear path following control systems for ocean vehicles," Ph.D. dissertation, IST/ISR, Lisbon, Portugal, Apr. 2002.

[27] J. Hespanha, D. Liberzon, and A. Morse, "Logic-based switching control of an non-holonomic system with parametric modeling uncertainty," *Syst. Control Lett.*, vol. 38, Special Issue on Hybrid Systems, no. 3, pp. 167–177, 1999.

[28] S. Hutchinson, G. D. Hager, and P. I. Corke, "A tutorial on visual servo control," *IEEE Trans. Robot. Autom.*, vol. 12, no. 5, pp. 651–670, Oct. 1996.

[29] ***[AU: Please provide referenced pages]***H. K. Khalil, *Nonlinear Systems*, 3rd ed. Upper Saddle River, NJ: Prentice-Hall, 1996.

[30] ***[AU: Please provide referenced pages]***M. Krstic, I. Kanellakopoulos, and P. Kokotovic, *Non-Linear and Adaptive Control Design*. New York: Wiley, 1995.

[31] ***[AU: Please provide page range]***L. Lapierre, D. Soetanto, and A. Pascoal, "Adaptive, non-linear vision-based path following control of a wheeled robot," in *Proc. 10th Mediterranean Conf. Control*, Lisbon, Portugal, Jul. 9–12, 2002.

[32] D. Liberzon, "Control using logic and switching, part 1: Switching in systems and control," in *Handout Notes of the CDC 01 Workshop*, September 4–7, 2001 [Online]. Available: http//:black.csl.uiuc.edu/liberzon

[33] A. Micaelli and C. Samson, "Trajectory tracking for a unicycle-type and two steering wheels mobile robots," Tech. Rep. INRIA n2097, Nov. 1993 [Online]. Available: http://www.inria.fr/rrrt/rr-2097.html

[34] C. Samson and A. Abderrahim, "Mobile robot control part 1: Feedback control of a non-holonomic mobile robot," Tech. Rep. INRIA n1281, Jun. 1991 [Online]. Available: http://www.inria.fr/rrrt/rr-1288.html

[35] ***[AU: Please provide referenced pages]***R. Sepulchre, M. Jankovic, and P. Kokotovic, *Constructive Non-Linear Control*. New York: Springler-Verlag, 1997.

[36] ***[AU: Please provide university and department]***C. Silvestre, "Multi-objective optimization theory with application to the integrated design of controllers/plants for autonomous vehicle," Ph.D. dissertation, Lisbon, Portugal, Jun. 2000.

[37] J. J. Slotine and W. Li, *Applied Non-Linear Control*. Englewood Cliffs, NJ: Prentice-Hall, 1995, pp. 125–128.

[38] ***[AU: Please provide page range]***D. Soetanto, L. Lapierre, and A. Pascoal, "Path-following control for a non-holonomic mobile robot with parametric modeling uncertainties," in *Proc. Eur. Control Conf.*, Cambridge, U.K., Sep. 1–4, 2003.

[39] ***[AU: Please provide page range]***D. Soetanto, L. Lapierre, and A. Pascoal, "Non-singular path-following control of a unicycle-type vehicle in presence of parametric modeling uncertainties," in *Proc. Int. Conf. Adv. Robot.*, Coimbra, Portugal, Jun. 30–Jul. 3 2003.

Lionel Lapierre received the Ph.D. degree ***[AU: In what field of study?]***from the University of Montpellier 2, Montpellier, France, in 1999.

Then, he joined the team of Prof. A. Pascoal within the European project FreeSub for three years. Since 2003, he has been with the Underwater Robotics Division, Laboratoire d'Informatique, de Robotique et de Microélectronique de Montpellier (LIRMM), Montpellier, France.

Bruno Jouvencel was born on February 3, 1955, in Paris, France. He graduated from the Electronical Engineering Department, Ecole Normale Supérieure, Cachan, France, in 1981 (Agrégation de Génie Electrique). He received the Ph.D. degree in perception systems for robotic manipulators in automatic control from Montpellier University, Montpellier, France***[AU: In what year?]***.

Currently, he is a Full Professor at Montpellier University and Researcher at the Laboratoire d'Informatique, de Robotique et de Microélectronique de Montpellier (LIRMM), Montpellier, France. In 2004, he was elected member of the National Committee, which evaluates French research laboratories in communication and information technologies (Section 07 of the Comité National de la Recherche Scientifique). For ten years, he has worked on the design, the command, and the perception of autonomous underwater vehicles. A first prototype TAIPAN 1 has been developed in 1998 and a second vehicle "H160" was conceived and realized in partnership with an industrial company.